(NASA-CR-170982) TURBINE BLADE TESTING METHODS Interim Report (Cincinnati Univ.) 80 p HC A05/MF A01 CSCL 21E

N84-18201

Unclas
G3/07 11821

INTERIM REPORT--NAS8-34503
TURBINE BLADE TESTING METHODS

Submitted to the

Structural Dynamics Research Division
Huntsville Research Center
National Aeronautics and Space Administration

by the

Department of Mechanical & Industrial Engineering
University of Cincinnati
Cincinnati, Ohio 45221
(513) 475-2738

INTERIM REPORT--NAS8-34503
TURBINE BLADE TESTING METHODS

Submitted to the

Structural Dynamics Research Division
Huntsville Research Center
National Aeronautics and Space Administration

by the

Department of Mechanical & Industrial Engineering
University of Cincinnati
Cincinnati, Ohio 45221
(513) 475-2738

NASA TURBINE BLADE MODAL TESTING STUDY

INTRODUCTION

The purpose of this study was to develop testing procedures which could be used to modal test turbine blades. The methods studied were methods which used and extended current modal testing procedures. An acoustical impacting testing method was perfected for testing small turbine blades.

REVIEW OF CURRENT TECHNOLOGY

The current procedures for testing blades can be divided into the conventional frequency response methods and the optical holographic methods. The technology investigated in this study was limited to conventional frequency response testing methods. The methods evaluated during the study were optimized according to blade size and mounting condition.

The most difficult testing situations were for small blades and/or blades mounted in discs with loose or non-linear boundary conditions. The study concentrated upon these measurement cases. The larger blades could be studied by conventional frequency response testing methods where a small accelerometer, strain gage or some other small displacement pickup is mounted on the blade and an exciter system(impactor or electro-mechanical exciter) is used to excite the modes of vibration.

The small blades, in general, had high natural frequencies and low modal mass. As a result, with current state-of-the-art transducers and exciter systems it is impossible to measure the eigenvalues and eigenvectors without significant errors due to the mass loading of the blade by the measurement system.

The smallest commercial exciters and impedance heads cause significant frequency shifts in those modes of vibration where the impedance heads contributed significant mass to the mode of vibration. In general, this would be modes of vibration which had significant motion normal to the force sensing direction of the impedance head. Since the impedance head could not measure these force, they were not considered in the frequency response measurements.

Also, the small blades are, in general, rather stiff and as a result it is difficult to excite the blades to high displacement values at the high natural frequency of the blades. Therefore, non-contacting displacement pickups are often not sensitive enough to make good measurements.

EXCITATION METHOD

An impacting method was chosen to excite the small blades since there is not mass loading effectwith this method. A small hand held impacting hammer was specially developed for the turbine

blade testing. A standard small PCB impacting hammer was purchased and used as the starting point for the hammer construction. The load cell was removed for this hammer and fitted with a very light weight epoxy reinforced handle. The mass of the hammer was reduced to a minimum in order to excite the frequency range of interest and to reduce the possibility of multiple impacts.

A special conical tip was machined on the tip by PCB. This is important for achieving repeatiable results on the frequency response measurements. Small impact caps can be used to reduce the frequency range inputs for impacting on larger or more flexible blades.

Unfortunately, for the small blades with the hand held impactor it requires good manual dexterity to operate the small hammer.

For even smaller blades, a small ball bearing can be used to impact the blades. For this case it was not possible to measure the input force. As a result, the frequency response of the blades could not be measured. The natural frequency could be measured from response spectra and estimates of mode shape could be estimated by the mass loading method described in Appendix A.

RESPONSE MEASUREMENTS

The response of the blades was measured whenever possible with a small accelerometer bonded at one point on the blades. The accelerometer was placed as close to the root of the blade as possible to minimize loading effects. It was important to pick a point where the modes of the blade could be measured. Small strain gages could also be used, however, for this work no strain gages were evaluated. In most applications it would not be necessary to have calibrated frequency response measurements since only the eigenvalues and eigenvectors would be the desired measurement result.

Non-contact probes were evaluated for measuring the response. Eddy current displacement probes were evaluated, but due to the small vibration levels and the difficulty of mounting the probes, they were not practical without constructing a special fixture for mounting and possibly scanning the probe. Optical displacement probes may be practical but were not evaluated during this contract because they were not available to the University. Again it would be necessary to have a probe positioning fixture.

Microphones were found to be very practical for measuring the response of the small blades. They are very sensitive to high frequency vibration of the blades particularly if the blades are lightly damped. Also, the positioning of the microphone is not critical. A great deal of work was spent on developing the microphone measurement method. A detailed analysis of this method is presented in Appendix B. The primary disavantage of the microphone method is that ambient noise can cause problems. Special filters may be required to filter out high background

noise problems. Also, there are some modes which are not good radiators of noise. Acoustical modes in the testing environment can be important, as a result, an anechoic chamber is the ideal testing environment.

IMPACTOR DESIGN AND EVALUATION

The design of the impactor is shown in Figure 1. A light weight handle was designed and modally tuned. The hammer was calibrated using a small Quixote Measurement Dynamics hammer calibrator. A typical calibration curve is shown in Figure 2. The hammer could be used to a frequency of 30,000 Hz. or greater if impacting on a hard surface.

MICROPHONE

A B&K one inch sound level microphone was used to measure the sound radiated by the blade under impacting conditions.

TEST EQUIPMENT

A HP 5423A Structural Dynamics Analyzer was used to make the impact measurements. Mode shapes and natural frequency could be determine directly with the 5423 for the data taken with small accelerometers. Due to the time delays present with the microphone, the curve fitting in the 5423 was not adequate. The data was either transferred to a HP 9816 desk top computer or the HP 5451C Fourier Analyzer system where it could be curve fit with the complex exponential curve fitting algorithm which can handle the time delay problem. Anatrol Corp.'s "PRISM" desk top modal software package was used to do the curve fitting in the 9816 and the University of Cincinnati "RTE MODAL" program was used in the 5451C system.

TEST PROCEDURE

Turbine Blade Boundary Condition.

The mounting condition for the turbine blade is very important. The easiest testing condition is a free-free condition, however, for most situations this is not acceptable. As a result in most cases the blade will be tested in a fixture which will duplicate the true mounting condition or by actually mounting the blade in its operating system.

The boundary condition at the root of the blade is very difficult to duplicate in the laboratory. In many cases, the blade is seated by centrifugal force during operation but in the laboratory it is free to move. This causes obvious problems with measuring the true operating frequencies and damping values. There are addition problems due to "rattles" and other non-linear behavior which make it difficult to obtain good frequency response measurements. This condition can be improved by pre-loading the blade in its mount which can be done by shimming the blade or by bonding the blade with a removable glue.

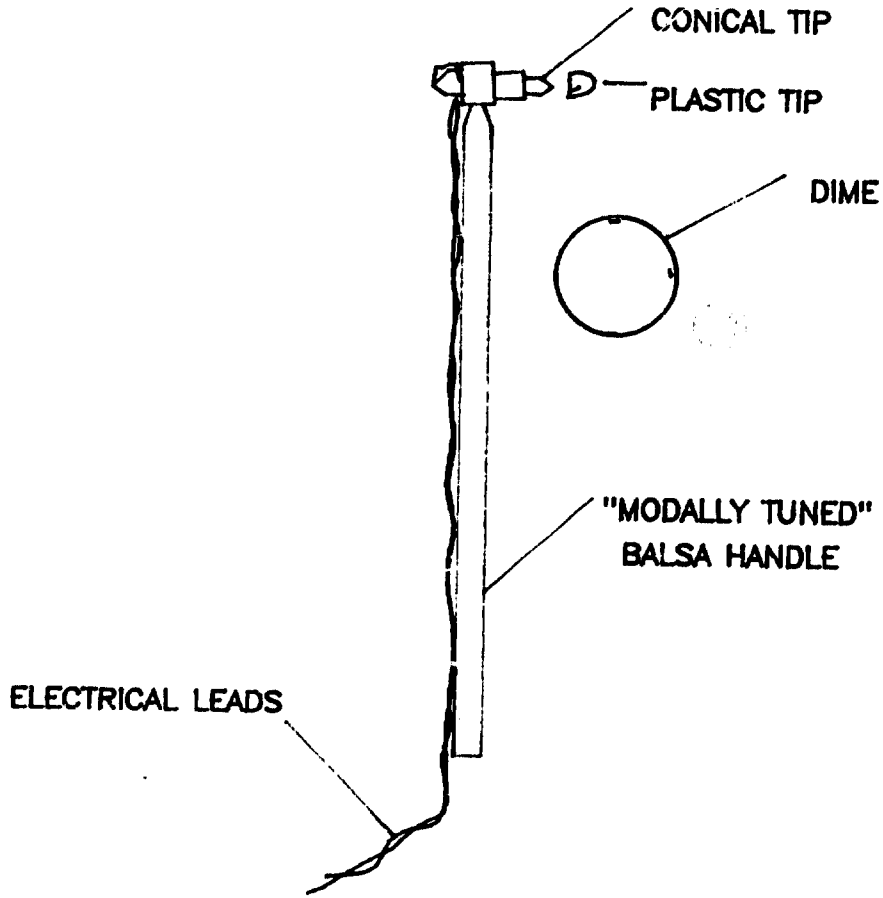

FIGURE 1 Schematic of Small Impact Hammer

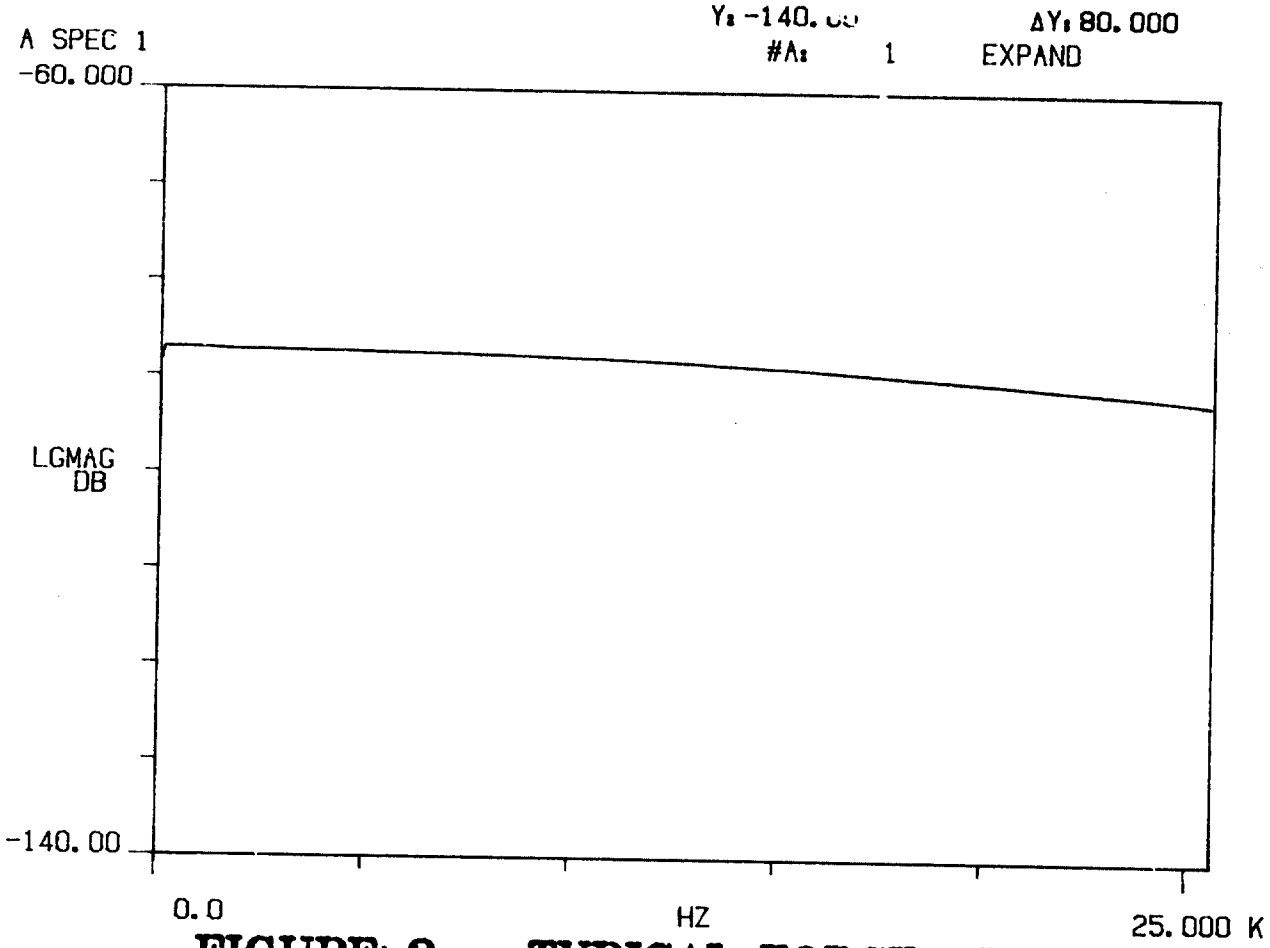

FIGURE 2 – TYPICAL FORCE SPECTRUM

If the purpose of the test is to compare with finite element results, then it is best not to measure the blade in the actual operating system since this condition has many modes of vibration associated with the total system and, in general, has many measurement problems due to non-linear behavior of the turbine system. The best approach is to model the system in a configuration which can be easily tested in the laboratory. This would be in a free-free condition or in a simple fixture which effectively mass loads the blade root. The mass loading is used to have forces acting on the blade root during the testing process.

Transducer Location

The location of the transducer should be picked, so that it is sensitive to those modes important in the evaluation of the blade, but minimizes the loading effects of the transducers. A position near the root of the blade is ideal since it offers reduced loading effects. Of course, several positions should be evaluated to mimimize the possiblity of missing an important mode. To evaluate the loading effects, two transducers can be used. One located at a fixed location on the blade and one which can be moved to likely mounting points on the blade. The fixed transducer can be used to measure the shift in frequency as the roving transducer is positioned. This shift will be representive of the shift present in the actual testing condition.

In the case of the microphone testing method the transducer is positioned at a point where the modes under investigation radiate a good sound pattern. It should be noted that whether the microphone is mounted in the near field or the far field is not important. However, in the near field the sound pressure levels of the radiated sound are higher and as a result the signal to noise ratio is higher which is a better signal processing condition. It is important in the near field that once the test is started no relative motion between the test object and the microphone exists. If the microphone is in the far field the relative position effects are minimized. In practice, the microphone has been placed approximately four inches from the blade being tested.

Excitation Considerations

The type of excitation is determined by the test setup and the size of the blade. The impacting method is better for the smaller blades. On the larger blades, impacting is also desireable, except for the cases where there are signbificant nonlinearities in the test article or it becomes necessary to zoom into a small frequency range. For these cases and electo-mechanical exciter system could be used.

Signal Processing

The type of signal processing that should be used is standard for the freequency response testing with the exception that for the microphone measurements it is important to minimized the effects of the time delay of the sound measurements. This can be done by using a pre-trigger delay between the force channel and the microphone channel.

For a test using an electro-mechanical exciter system, it is important to use signal processing and excitation methods to minimize the effects of "leakage". Force and exponential windows should be used for the impacting test.

Finite Element Analysis

Whenever possible it is good to have a finite element analysis performed on the turbine blade being tested. For extremely, small blades it is difficult to locate a large number of test points on the turbine blade. For these cases, the basic nature of the modes of vibration can be determined from the testing, and the finite element modes can be used to describe the modes. The natural frequencies obtained from the test can be used to adjust the finite element model. For these cases, it would be advisable to test the blade in two steps, a free-free test and a mounted test. The blade should be modelled with a finite element program in both conditions for comparison. The free-free test would be used to verify the turbine blade model and the finite element system model should be used to adjust the boundary conditions.

TEST RESULTS

A number of different turbine blades were tested during this study program. The blades sizes were varied from very small to large.

Test Setup

A typical photograph of the testing setup is shown in Figure 3. The equipment shown is the HP 5423A and the HP 9816 desk top computer. In Figure 4, a photograph of the impacting test on a larger blade is shown with a small accelerometer mounted on the blade. In Figure 5, the same blade is shown with the microphone being used as a pickup. The set-up typical of smaller blades is shown in Figure 6.

A typical test is shown in progress in Figure 7.

Frequency Response Measurements

Impact testing was primarily used during this testing program. A great deal of effort was spent on perfecting a testing method for small blades. A special hammer was constructed by rebuilding a standard small PCB impact hammer. A very light weight handle was constructed from epoxy coated balsa wood. This hammer was then

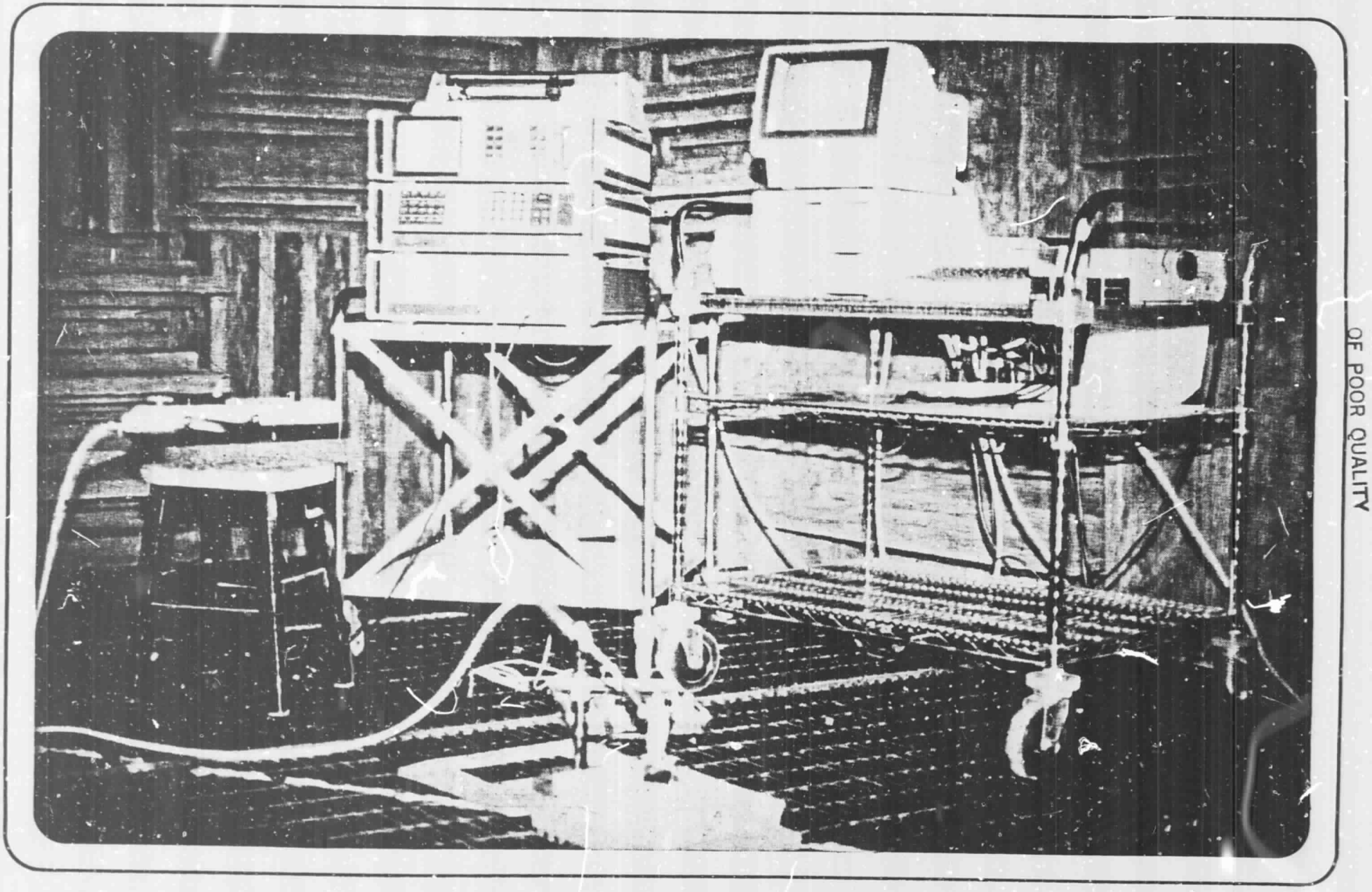

FIGURE 3 – TEST EQUIPMENT – HP5423A & HP9816

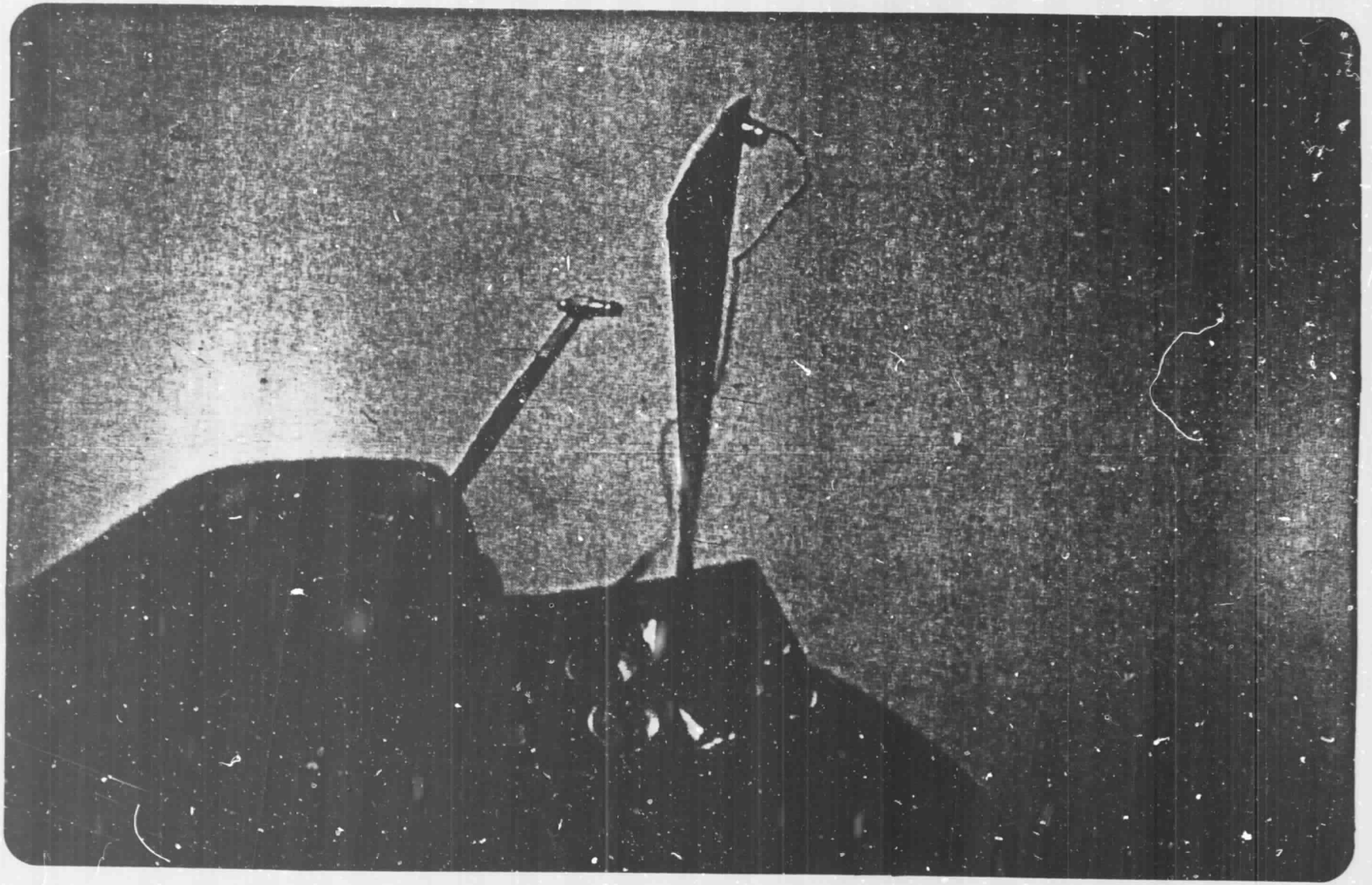

FIGURE 4 – TYPICAL TEST SETUP ON LARGE BLADE

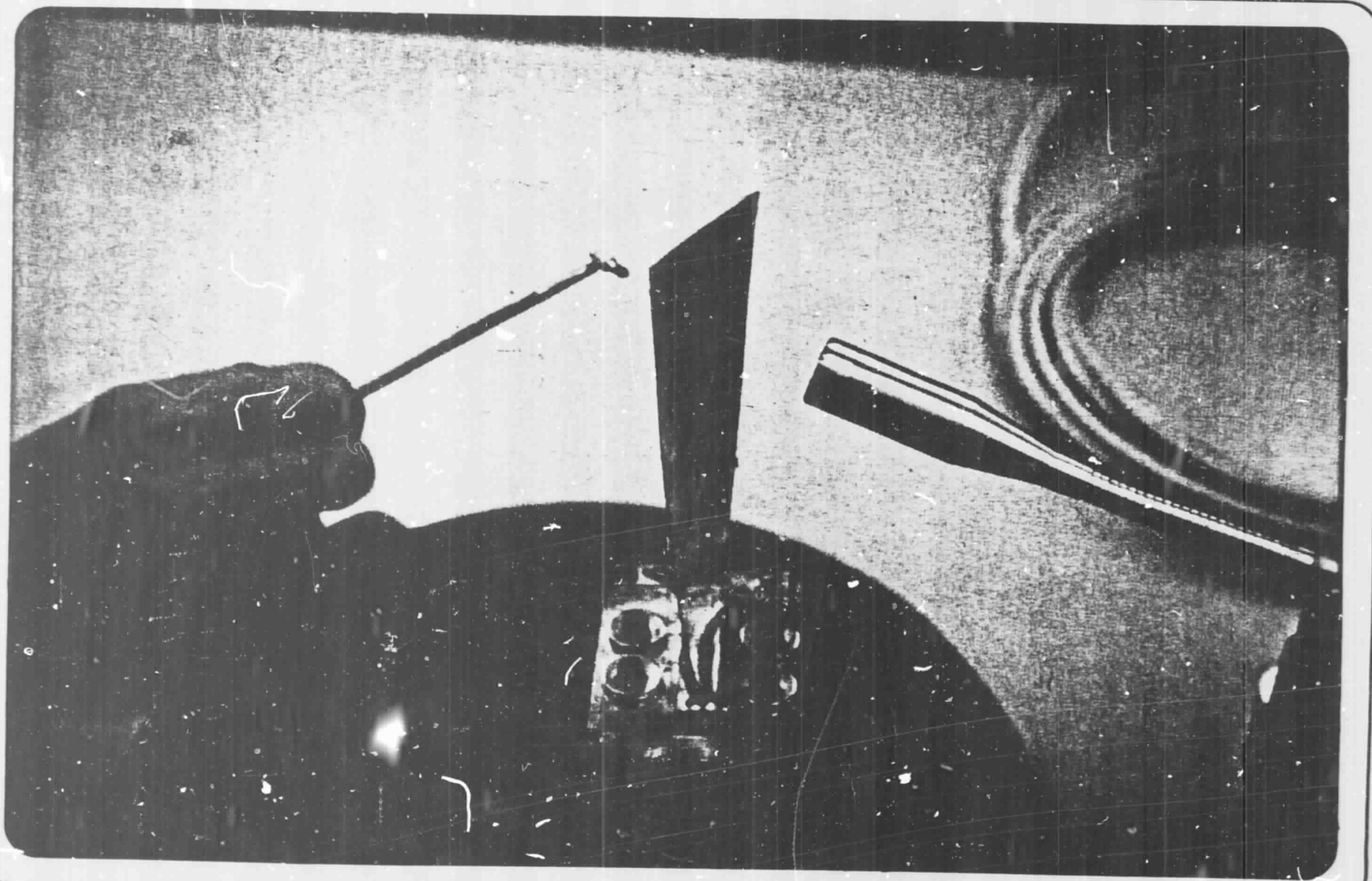

FIGURE 5 – TEST SETUP USING MICROPHONE

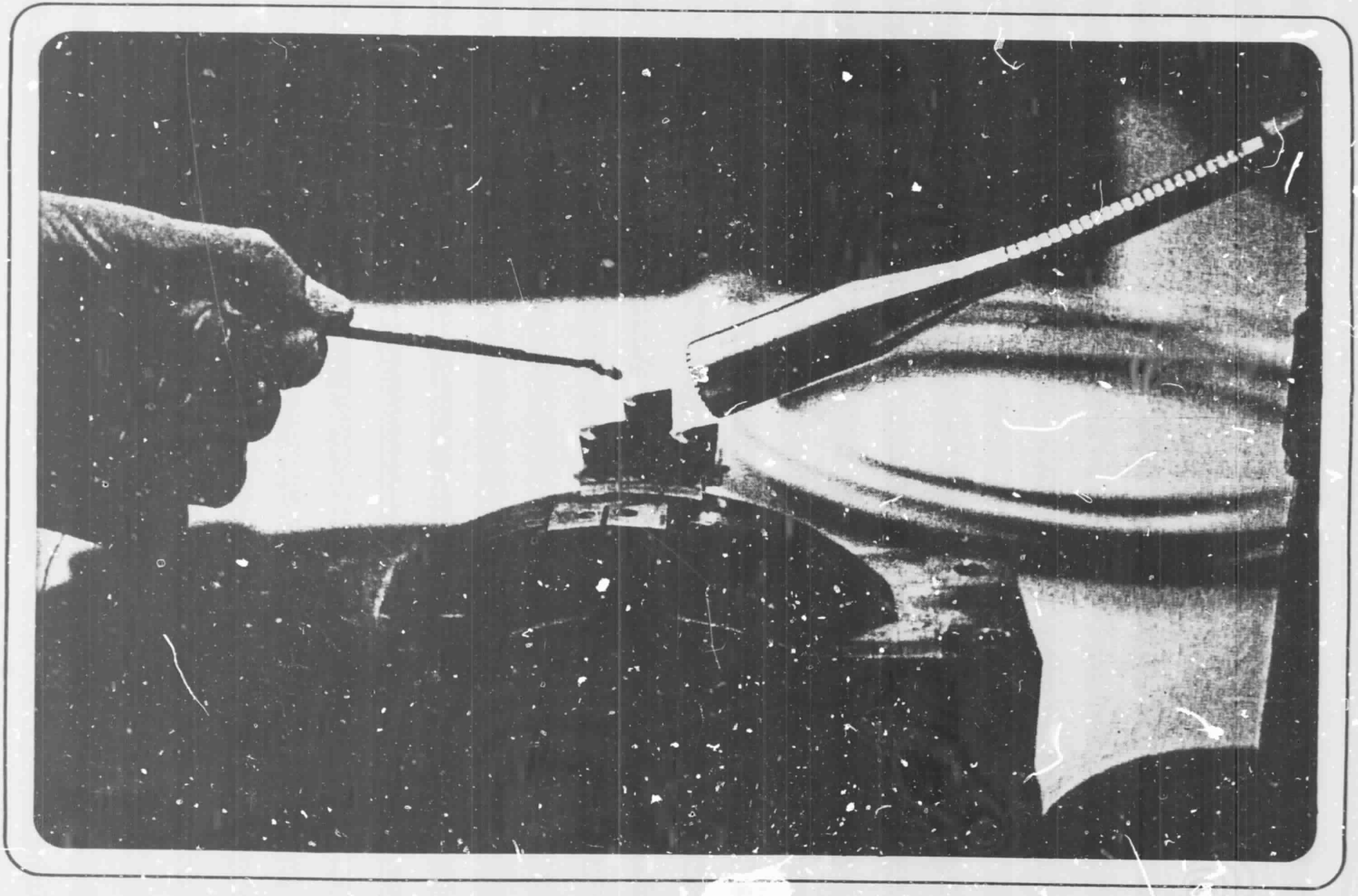

FIGURE 6 – TYPICAL SETUP FOR SMALL BLADES

FIGURE 7 – TYPICAL TEST IN PROGRESS

modally tuned to eliminate any hammer modes which would effect the force spectrum. The hammer has a special conical tip which improves the repeatablity of the force signal. A typical force spectrum is shown in Figure 8.

Frequency response measurements made on a small turbine blade with the small impact hammer are shown in Figure 9 and 10 for a driving point and cross measurement.

The small hammer can be used to measure frequency response functions with a maximum frequency of over 30,000 Hz. The actual frequency range is determined by the hardness of the contact zone between the hammer and the turbine blade.

It takes a person with good manual dexterity to use the hammer, therefore, it is important to practice before performing a functional test.

With practice, the frequency response measurements made with the small hammer gave excellent results even on the smallest blades tested.

Parameter Estimation

For the cases where an accelerometer is used, the standard single and multi-degree of freedom modal parameter estimation algorithms can be used to estimate the modal parameters (frequency, damping, and mode shapes).

For the microphone cases it is necessary to use a method which has the ability to handle the phase shift due to the time delay caused by the propagation of the sound signal. A pre-trigger delay can be used to reduce this effect and the standard methods of analysis can often be used. The complex exponential algorithm can be used to obtain the desired results even with significant delays present in the data. A modified parameter estimation method was developed which can take the time delay directly into consideration. This method is desribed in detail in Appendix A.

Typical Results

A large number of blades were tested as part of this study. A set of typical results is shown in Appendix B. A comparison between standard testing methods and the acoustical method is shown.

For very small blades the difficulty is locating points on the blade. In these cases only enough points were taken to correlate the results with the finite element results.

For cases where a large number of blades are mounted on a turbine disc, a problem with group modes can develop. A group mode is one where in a very narrow frequency range, a large number of modes of the same nature exist. This is caused by the large number of blades and is exaggerated by the slightly different

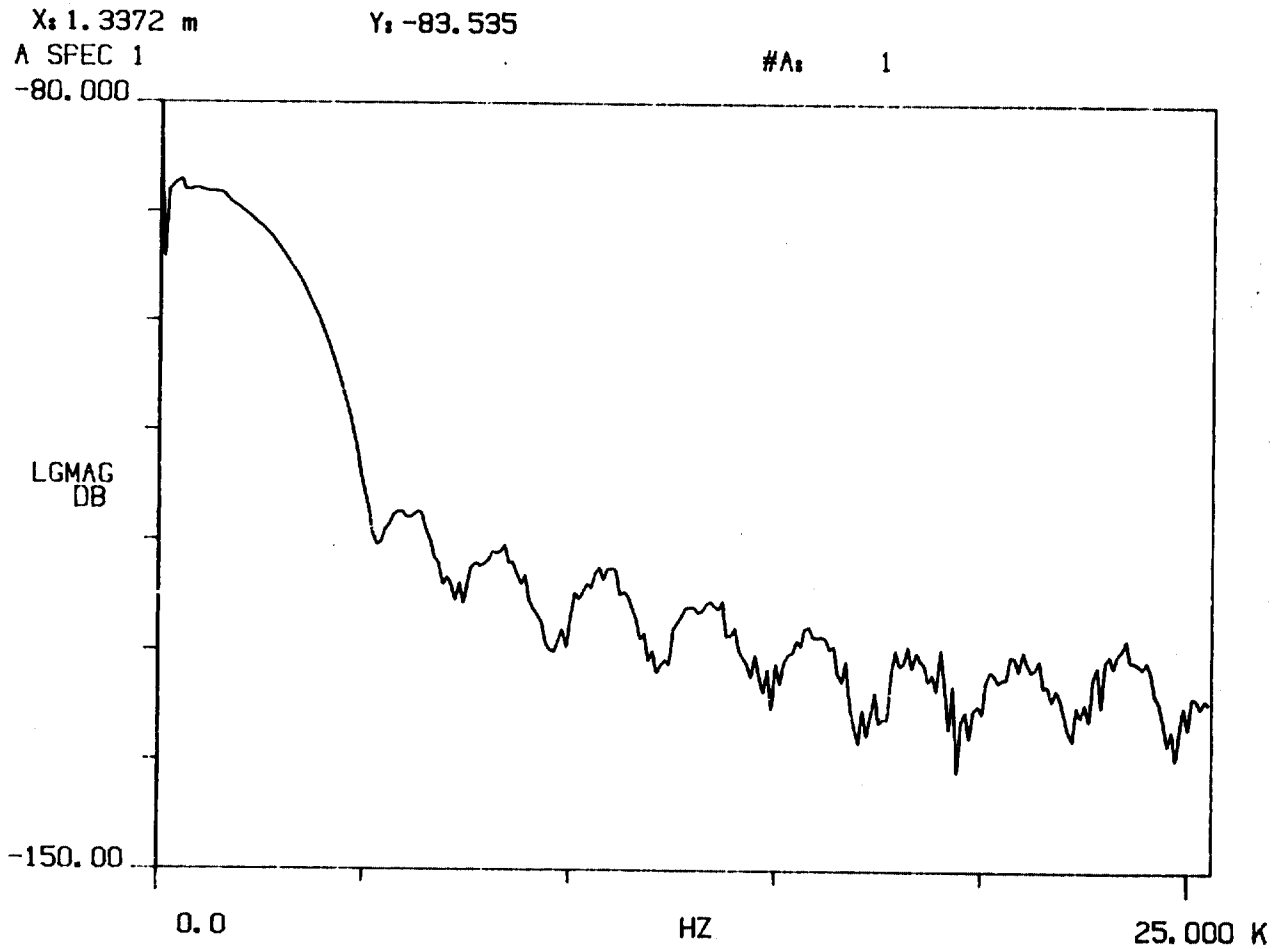

FIGURE 8 – TYPICAL FORCE SPECTRUM – PLASTIC TIP

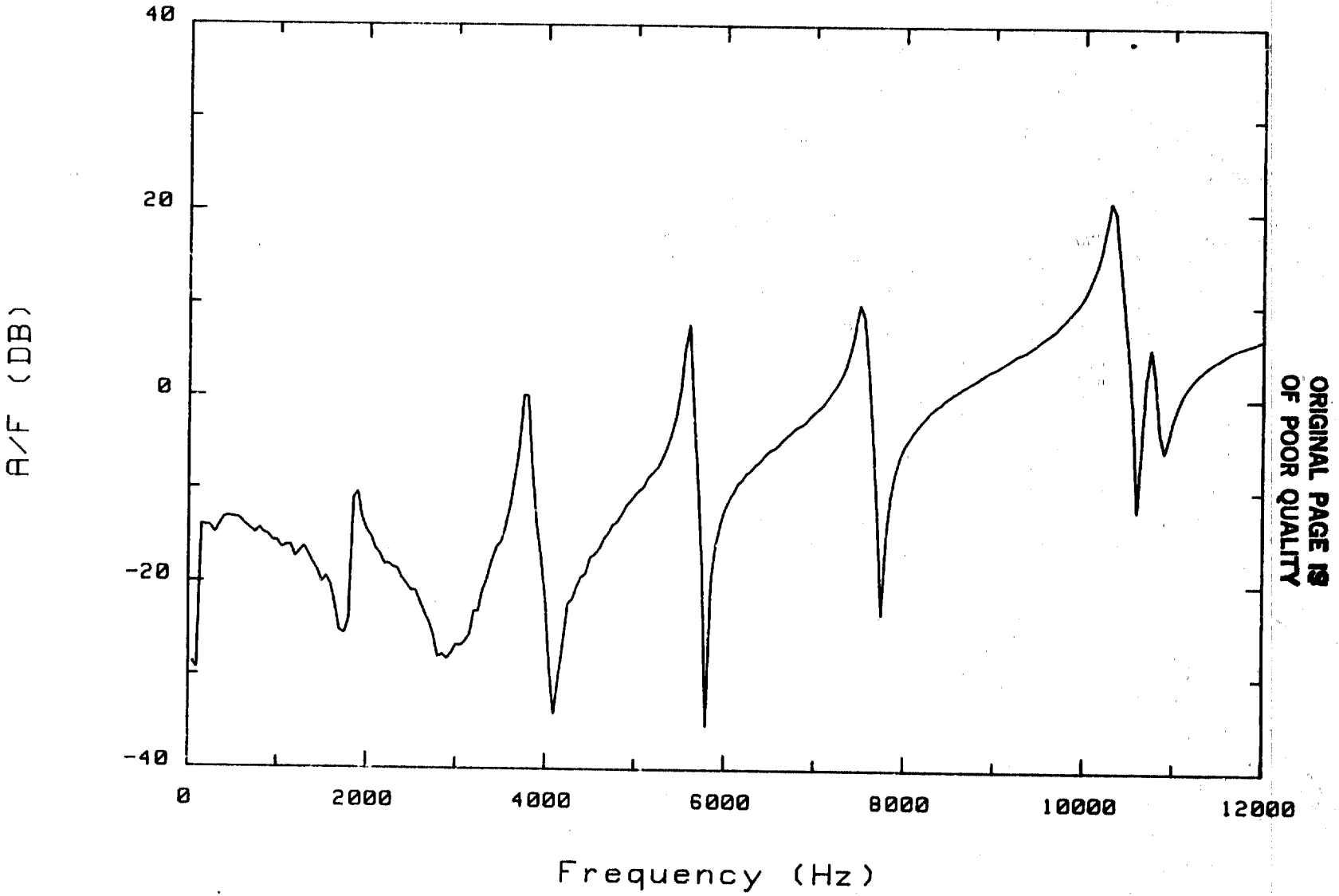

FIGURE 9 – TYPICAL DRIVING POINT MEASUREMENT

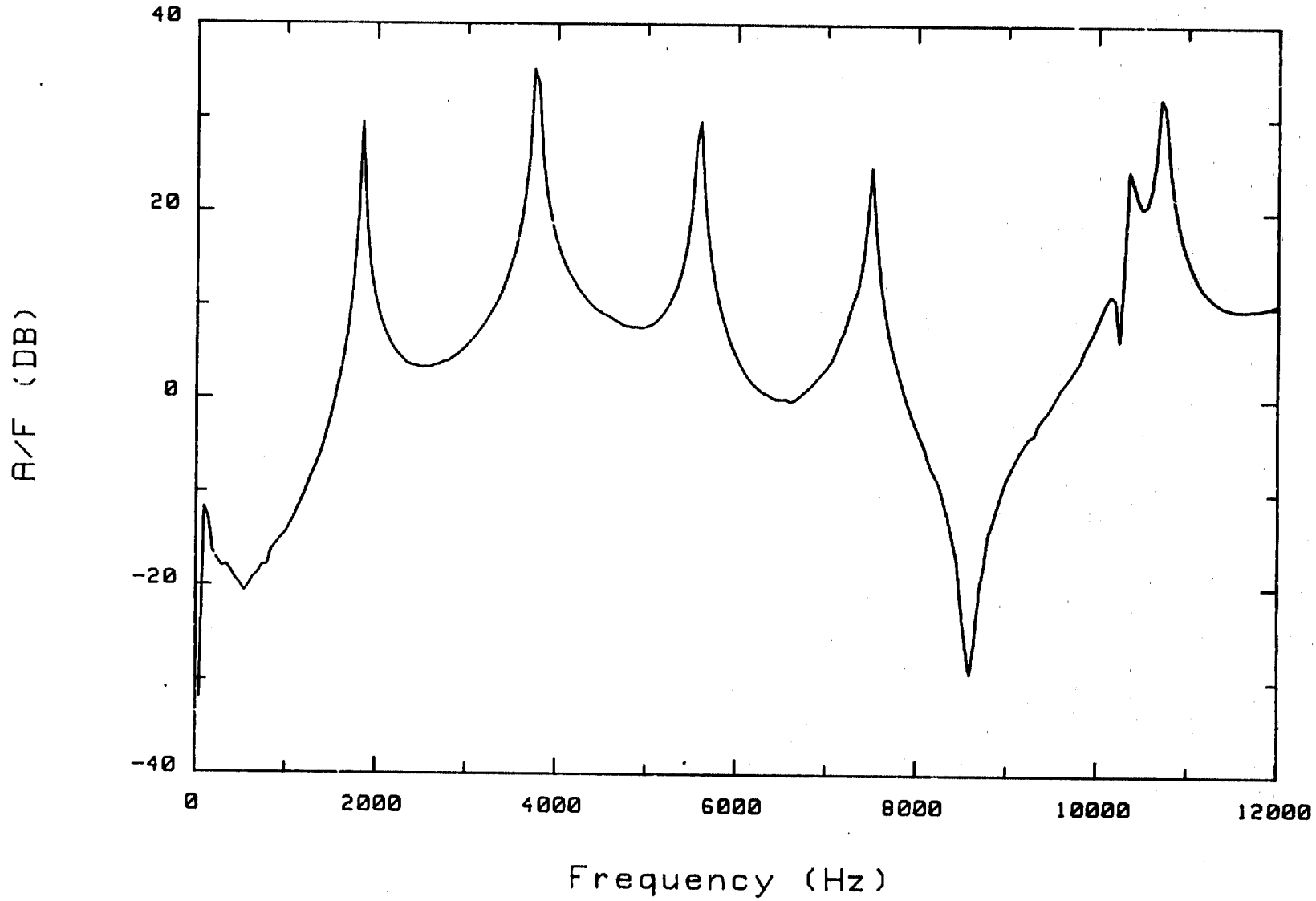

FIGURE 10 – TYPICAL CROSS MEASUREMENT

tuning of each individual blade on the disc. For these cases, it is necessary to zoom in on the frequency range, to separate the closely spaced modes. For close zoom ranges it is often difficult to obtain good frequency response measurements with impact testing. For these cases, a test where the turbine disc is excited with an electro-mechanical device is a better solution because the energy can be concentrated in the frequency range of interest. By exciting on the turbine disc, the loading effects of the exciter system are minimized from the test considerations. Care must be taken to locate a point on the turbine disc which will excite the modes of interest.

SUMMARY

A method has been developed for testing small turbine blades. This method uses a non-contact microphone and impact testing to eliminate the transducer loading problems associated with conventional testing methods. For larger blades, the more conventional testing methods work well.

APPENDIX A

TURBINE BLADE TESTING

D.5 ONE CHANNEL FREQUENCY RESPONSE AND MODE PARAMETER MEASUREMENTS

In order to measure the frequency response of a system, it is necessary to measure the input signal and output response of a system (see Section IV of Appendix A). There are cases in which it is either impossible or inconvenient to measure the input of a system, or the data processing equipment is only available for processing one channel of data. In this case, an approximation of the frequency response and approximate mode coefficient can be obtained by measuring the response spectrum only. The measurement is made by altering the test system by adding mass or connecting some other structure to the test system at selected points and then measuring the shift in natural frequency of the new system.

The simplest method is that of adding mass to the system at a predetermined point. The driving point frequency response at the point (A) where the mass has been added to the structure can be written as:

$$\frac{X_A}{F_A} = H_{AA} = \sum_{i=1}^{n} \frac{(\phi_A)_i^2}{[1-\frac{\omega}{\omega_i})^2+2\zeta_i\frac{\omega}{\omega_i}j]} \qquad D.5.1$$

for a system which can be approximated by real normal modes. Or rewriting in terms of effective stiffness, mass, and damping:

$$H_{AA} = \sum_{i=1}^{n} \frac{1}{K_{A_i}-M_{A_i}\omega^2+C_{A_i}\omega j} \qquad D.5.2$$

where ψ_{A_i} ∿ eigenvector

ω_i ∿ natural frequency of i^{th} mode

P_i ∿ damping coefficient of i^{th} mode

K_{A_i} ∿ effective stiffness of i^{th} mode at point a

m_{A_i} ∿ effective mass of i^{th} mode at point a

C_{A_i} ∿ effective damping of i^{th} mode at point a

The frequency response at point A which is modified by connecting an additional system is given by the following expression:

$$(H_{AA})_f = \frac{(H_{AA})_i}{1+\frac{(H_{AA})_i}{H_c}} \qquad \text{D.5.3}$$

where $(H_{AA})_i$ = initial frequency response at point A

$(H_{AA})_f$ = final frequency response after system is altered

H_c = frequency response of connecting system

$= \frac{1}{\omega^2 m}$ for pure mass D.5.4

m = added mass

Substituting D.5.4 and D.5.2 into equation D.5.3, the resulting equation is obtained:

$$(H_{AA})_f = \left(\frac{X_A}{F_A}\right)_f = \sum_{i=1}^{n} \frac{1}{[K_{A_i} - (m_{A_i} + m/\omega^2 + C_{A_i}\omega_j]} \qquad \text{D.5.5}$$

The natural frequency of the original system for the i^{th} mode is:

$$\omega_i = \sqrt{\frac{k_{Ai}}{m_{Ai}}} \qquad \text{D.5.6}$$

and for the modified system is:

$$\omega_{i_f} = \sqrt{\frac{k_{Ai}}{m_{Ai}+m}} \qquad \text{D.5.7}$$

Therefore, equation D.5.6 and D.5.7 can be solved for K_{ai} and m_{ai} in terms of the measured frequencies and the added mass (m) or:

$$m_{Ai} = m\left(\frac{1}{\frac{\omega_i^2}{\omega_{if}^2} - 1}\right) \qquad \text{D.5.8}$$

and

$$k_{Ai} = m\left(\frac{\omega_{if}^2}{\omega_i^2 - \omega_{if}^2}\right) \qquad \text{D.5.9}$$

The damping term can be measured from the half-power points, rate of decay or by any number of different techniques. Once m_{ia}, K_{ia}, and C_{ia} are known, then the frequency response of the driving point can be estimated from equation D.5.2. If the mass is moved from point to point on the structure, then the eigenvector or mode shape can be obtained from

The acoustic pressure is also expressed by $jw\rho$, then by formula (3) , the acoustic pressure is

$$P_A = jw\rho \frac{1}{2\pi} V \iint_S \frac{e^{-ikR}}{R} dS \tag{4}$$

Suppose that the structure surface is composed of these piston sources , the acoustic pressure is

$$P_A = \sum_{m=1}^{L} p_m = jw\rho \sum_{m=1}^{L} \frac{1}{2\pi} V_m \iint_S \frac{e^{-ikR_m}}{R_m} dS_m \tag{5}$$

When a force is applied at a point i on the structure , the velocity(V_m) of the piston can be expressed as follows.

$$V_m = jwH_{mi}F_i \tag{6}$$

$$H_{mi} = \sum_{r=1}^{\infty} \frac{u_m u_i}{a_r(j\omega - p_r)} + \frac{u_m^* u_i^*}{a_r^*(j\omega - p_r^*)} \tag{7}$$

: frequency response function

Then formula (5) becomes

$$\begin{aligned} P_A &= -w^2 \frac{\rho}{2\pi} \sum_{m=1}^{L} H_{mi} \cdot F_i \iint_S \frac{e^{-ikR_m}}{R_m} dS_m \\ &= -w^2 \frac{\rho}{2\pi} \sum_{m=1}^{L} \left\{ \sum_{r=1}^{\infty} \frac{u_m u_i}{a_r(j\omega - p_r)} + \frac{u_m^* u_i^*}{a_r^*(j\omega - p_r^*)} \right\} \cdot F_i \iint_S \frac{e^{-ikR_m}}{R_m} dS_m \\ &= -w^2 \frac{\rho}{2\pi} \sum_{r=1}^{\infty} \left\{ \frac{u_i \left(\sum_{m=1}^{L} u_m \iint \frac{e}{R_m} dS_m \right)}{a_r(j\omega - p_r)} + \frac{u_i^* \left(\sum_{m=1}^{L} u_m^* \iint \frac{e}{R_m} dS_m \right)}{a_r^*(j\omega - p_r^*)} \right\} \cdot F_i \end{aligned} \tag{8}$$

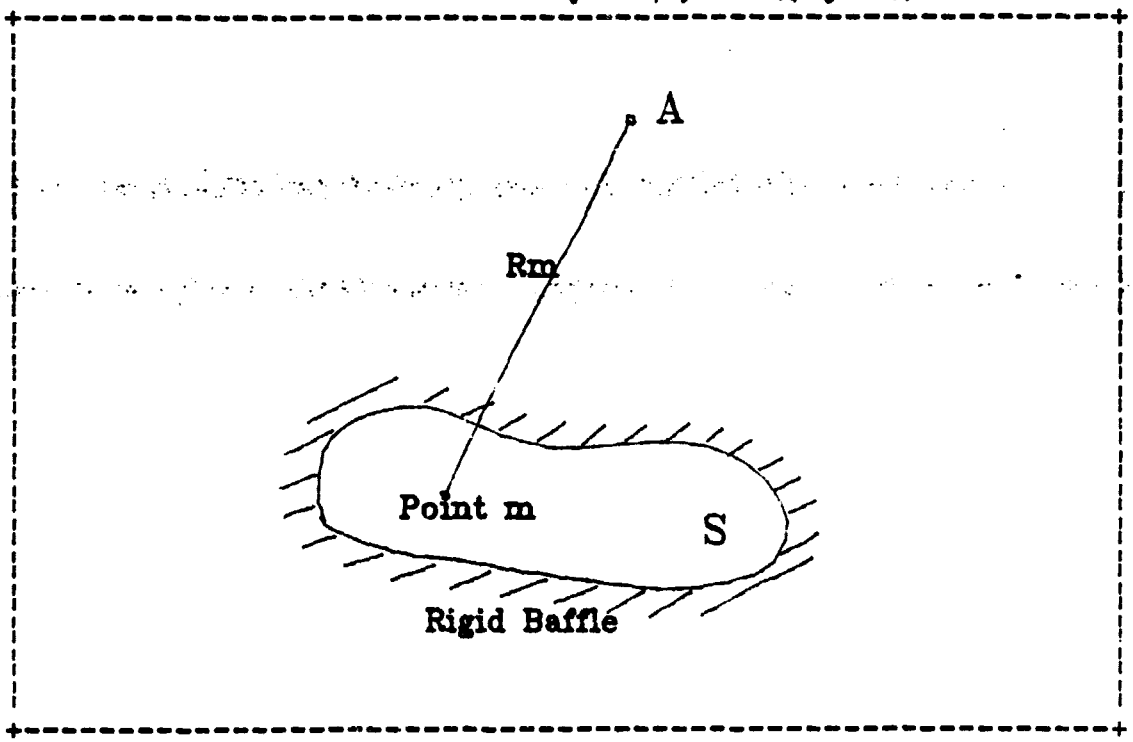

Fig.3 RADIATION MODEL

Laplace program (User program Y70, see Appendix B) was then used to calculate the natural frequencies and damping coefficients in the zoom transformed range. The procedure gave very repeatable results for the natural frequency measurement. For example, the second bending mode frequency was at 4328 Hz, and the standard deviation was only 0.25 Hz for the measurement. In Figure D.5.1 the first three measured mode shapes are given for the beam. As can be seen from this figure, reasonable mode shapes are obtained.

The technique also has application for cases where two channel measurements can be made to obtain good scaling values for eigenvectors. A known mass can be added to the system and the change in the natural frequency can be determined and used to compute the effective mass or stiffness of a mode of vibration. A series of masses can be added and the effective mass can be determined in a least square sense from these series of measurements for improved accuracy.

The rigid body modes of a complex system can be determined by moving a known mass around the system and calculating the effective mass of the six rigid body modes. From the six rigid body modes, the location of the center of gravity and the rotary moments of inertia can be determined.

D.6 MICROPHONE MODE SHAPE MEASUREMENTS

Several times during the thesis project a microphone was used with impact testing for determining the natural

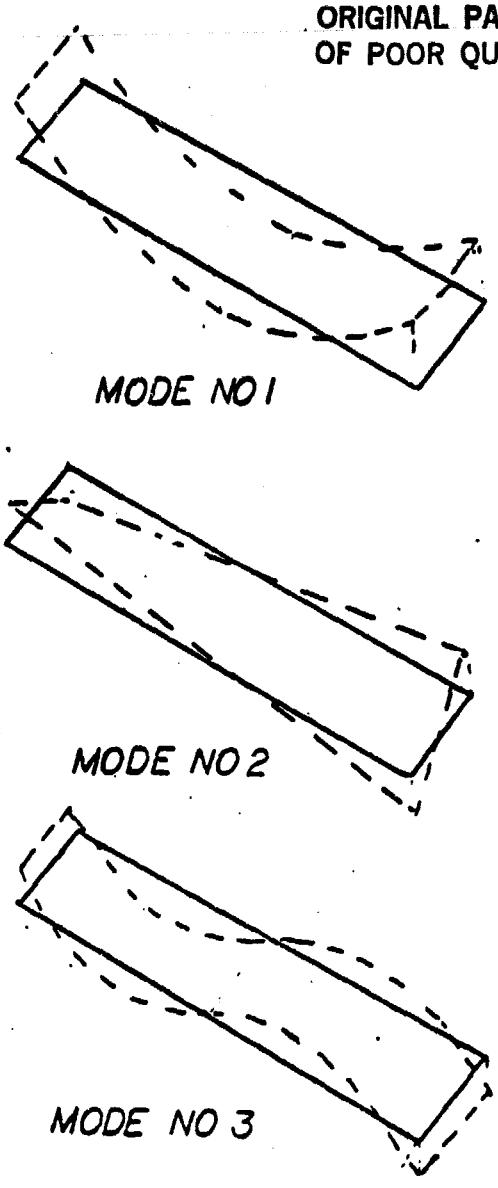

FIGURE D.5-1 MODES 1-3 FOR GRAPHITE-EPOXY BEAMS

frequency and damping factors for small lightly damped systems. Since the microphone didn't contact the part being tested, it never loaded the part and the measured frequency and damping factor were accurate. (see Appendix D.5). Very good mode shapes could also be determined by fixing the microphone in space and using imparting techniques to measure the mode shape vibration of the part. The mode shape was determined by moving the impactor from point to point on the part being tested. The level of vibration for each mode varied with the impact point by an amount proportional to the modal coefficient at that point. The microphone measured the sound radiated by the part which is a measure of the vibration of the part. Since the microphone is positioned remotely from the part, there is a phase delay in the resulting frequency response; therefore, circle fitting or Laplace fitting should be used to measure the modal coefficient.

APPENDIX B

TURBINE BLADE TESTING

Table of Contents

LIST OF FIGURES

LIST OF TABLES

ABSTRACT

The modal parameters estimation technique for the frequency response function which is the ratio of an acoustic signal to an input force was developed in this paper. By this technique we could estimate frequencies ,dampings ,modal vectors and modal mass. In modal analysis the modal mass cannot be estimated without a driving point measurement. But this technique can handle the modal mass without a driving point measurement.

This paper includes two examples (Turbine blade, T-plate). The results were compared with the results by modal analysis and it had a good correlation. Moreover, in order to check the accuracy of the results two attempts were performed. One is that the frequency response functions at a different microphone position were predicted. Another is the prediction of the frequency response function of the modified structure with some amount of mass. Both had good results.

Notation in this paper

φ	=	Velocity potential
S	=	Area of the structure surface
R	=	Distance from the each point on the structure to the microphone
l	=	Distance between the structure and the microphon??
w	=	Frequency(=2πf)
w_{dr}	=	Damped natural frequency of r-th mode
w_r	=	Undamped natural frequency of r-th mode
C	=	Sound speed
k	=	Wave number (w/C)
Pr	=	Eigen value of the r-th mode
δ_r	=	Delay rate of r-th mode (damping)
N	=	Number of points measured on the structure
M	=	Number of modes of interest
L	=	Number of points which radiate the noise to the microphone
r	=	Mode number
ρ	=	Density of the air
P	=	Acoustic pressure
G	=	Experimental frqeuency response
H	=	Analytical frequency response
Y	=	Residual mass
Z	=	Residual flexibility
ξ_r	=	Damping factor

INTRODUCTION — CHAPTER 1

When one efficiently reduces the noise from the structures , the technique to determine the dynamic characteristics of the structure and predict the radiated noise is required. So far some papers have been devoted to this area but these papers have used the method as in Figure 1. The drawbacks of this method are that the noise radiation cofficiency must be predicted , because it is very difficult to predict for the complicated structures and modes.

In order to resolve this problem , the technique in this paper determines directly the characteristics of a structure using an acoustic signals as illustrated in Figure 2. By this technique the radiated noise can be predicted without the calculation of the noise radiation cofficiency.

Moreover , the merits of this technique are,

1) It is not necessary to put the accelrometer onto the structure.
2) Directly the mode which contributes much to the radiated noise can be found.
3) It is not necessary to calculate the noise radiation cofficiency.

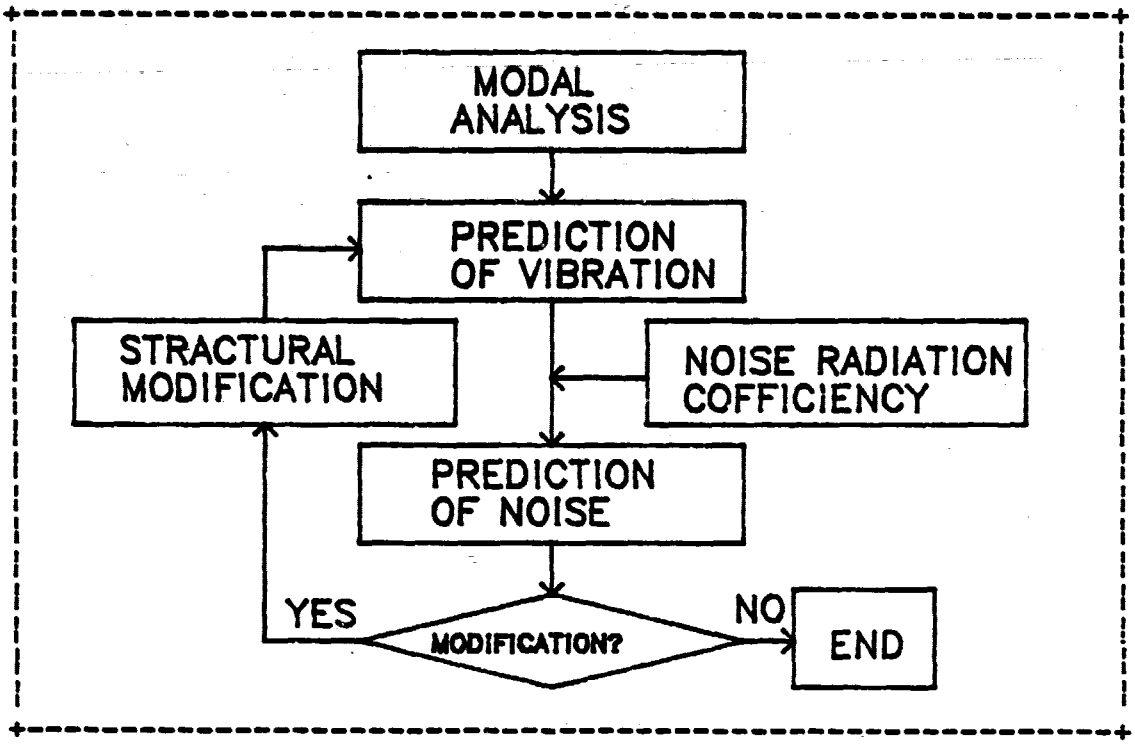

Fig.1 Flow of the noise reduction

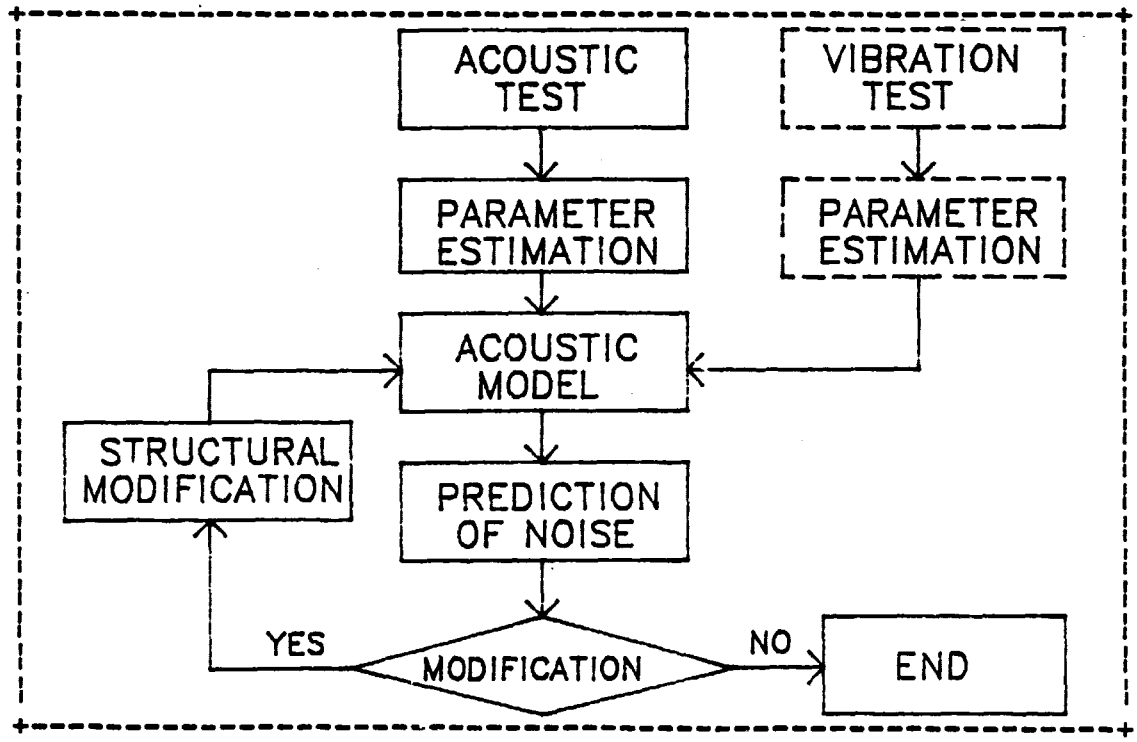

Fig.2 Flow of the noise reduction

THE THEORY OF SOUND	CHAPTER 2

2.1 THE RADIATION OF SOUND

In tkis paper the radiation by a plane piston will be used as the acoustic model. But the details will not be discussed here if anyone wants to know the details , please refer to the references [1],[2],[3].

The radiation of a piston can be analysed by a general method if the velocity potential and its normal derivative are known on the bounding surface.

The velocity potential of a point source with strength $(\frac{\partial \varphi}{\partial n})_S dS$, radiating into a solid angle 2π is

$$d\varphi = -\frac{1}{2\pi}(\frac{\partial \varphi}{\partial n})_S \frac{e^{-jkR}}{R} dS. \qquad (1)$$

If these point sources exist in the plate and outside these sources is occupied by a rigid baffle , the velocity potential at a point A (Figure 3) is obtained by adding the potentials d of the individual point sources over the area S,with the retarded phase expressed by the factor exp(-jkR). that is

$$\varphi_A = -\frac{1}{2\pi}\iint_S (\frac{\partial \varphi}{\partial n})_S \frac{e^{-jkR}}{R} dS \qquad (2)$$

Moreover , if the velocity of the piston surface is V , $V = -(\frac{\partial \varphi}{\partial n})_S$, then the potential is expressed as (3).

$$\varphi_A = \frac{1}{2\pi} V \iint_S \frac{e^{-jkR}}{R} dS \qquad (3)$$

The acoustic pressure is also expressed by $jw\rho$, then by formula (3) , the acoustic pressure is

$$P_A = jw\rho \frac{1}{2\pi} V \iint_S \frac{e^{-ikR}}{R} dS \tag{4}$$

Suppose that the structure surface is composed of these piston sources , the acoustic pressure is

$$P_A = \sum_{m=1}^{L} p_m = jw\rho \sum_{m=1}^{L} \frac{1}{2\pi} V_m \iint_S \frac{e^{-ikR_m}}{R_m} dS_m \tag{5}$$

When a force is applied at a point i on the structure , the velocity(V_m) of the piston can be expressed as follows.

$$V_m = jwH_{mi}F_i \tag{6}$$

$$H_{mi} = \sum_{r=1}^{\infty} \frac{u_m u_i}{a_r(j\omega - p_r)} + \frac{u_m^* u_i^*}{a_r^*(j\omega - p_r^*)} \tag{7}$$

: frequency response function

Then formula (5) becomes

$$\begin{aligned} P_A &= -w^2 \frac{\rho}{2\pi} \sum_{m=1}^{L} H_{mi} \cdot F_i \iint_S \frac{e^{-ikR_m}}{R_m} dS_m \\ &= -w^2 \frac{\rho}{2\pi} \sum_{m=1}^{L} \left\{ \sum_{r=1}^{\infty} \frac{u_m u_i}{a_r(j\omega - p_r)} + \frac{u_m^* u_i^*}{a_r^*(j\omega - p_r^*)} \right\} \cdot F_i \iint_S \frac{e^{-ikR_m}}{R_m} dS_m \\ &= -w^2 \frac{\rho}{2\pi} \sum_{r=1}^{\infty} \left\{ \frac{u_i \left(\sum_{m=1}^{L} u_m \iint \frac{e}{R_m} dS_m\right)}{a_r(j\omega - p_r)} + \frac{u_i^* \left(\sum_{m=1}^{L} u_m^* \iint \frac{e}{R_m} dS_m\right)}{a_r^*(j\omega - p_r^*)} \right\} \cdot F_i \end{aligned} \tag{8}$$

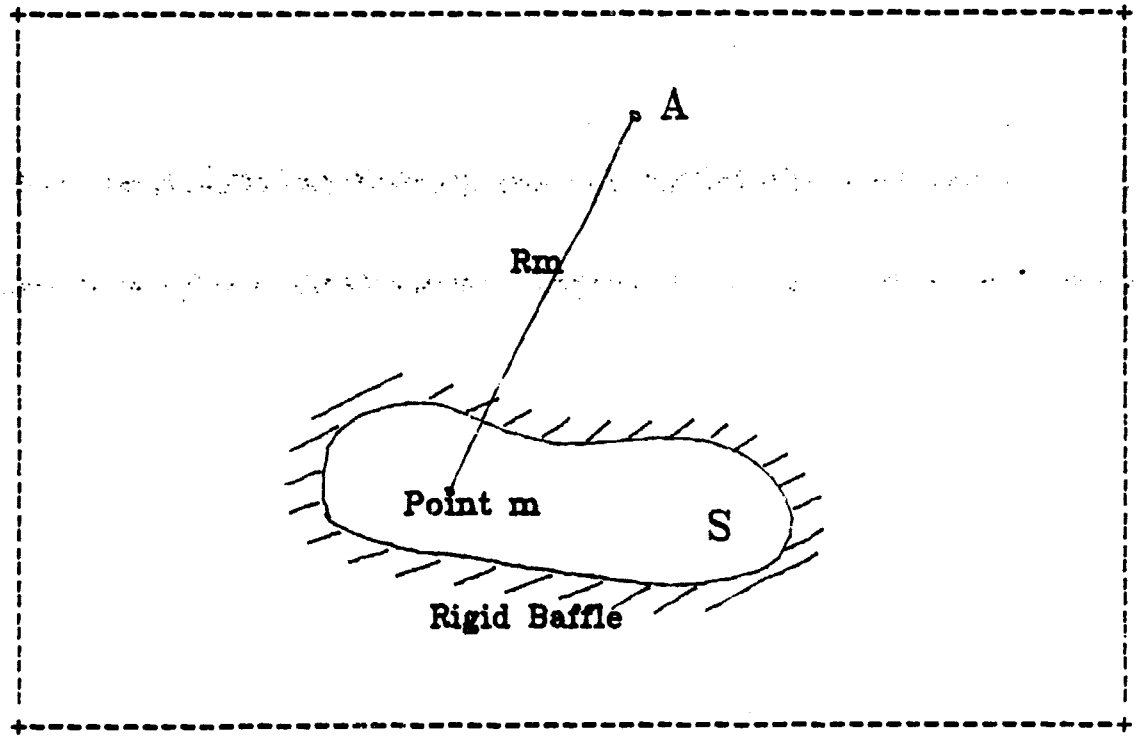

Fig.3 RADIATION MODEL

2.2 FREQUENCY RESPONSE FUNCTION

2.2.1 FAR FIELD MODEL

In the far field model , the following condition can be assumed.

$$R \gg d \tag{9}$$

Therefore, $R = R_m = l = \text{cost.}$

$$\exp(-jkR) = \exp(-jkl)\exp(-jk\Delta R) \tag{10}$$

Where, $R = u\sin(\theta)\cos(\Phi)$

Formula (8) becomes

$$p_A = -w^2 \frac{\rho}{2\pi} \sum_{r=1}^{\infty} \left\{ \frac{u_i (\Sigma u_m \iint e^{-jk\Delta R} dS)}{a_r (j\omega - p_r)} + \frac{u_i^* (\Sigma u_m^* \iint e^{-jk\Delta R} dS)}{a_r^* (j\omega - p_r^*)} \right\} \frac{e^{-jkl}}{l} F \tag{11}$$

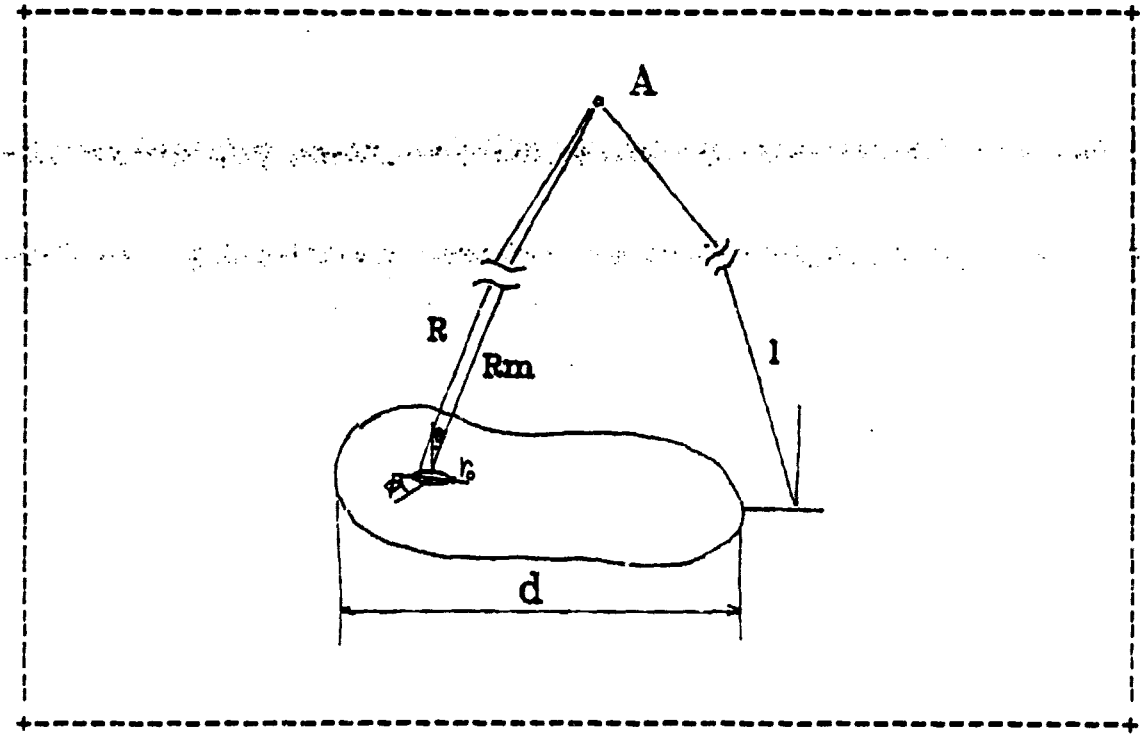

Fig.4 ACOUTIC RADIATION MODEL(FAR FIELD)

Putting $k u \sin\theta = z'$ and $k r_0 \sin\theta = z_0'$, and using relations from Bessel function theory, we get

$$\begin{aligned}\exp(-jku\sin\theta\cos\phi)\,dS &= \int_0^{r_0} u\,du \int_0^{2\pi} \exp(-jku\sin\theta\cos\phi)\,d\phi \\ &= 2\pi \int_0^{r_0} u J_0(z')\,du \\ &= \frac{2\pi}{(k\sin\theta)^2} \int_0^{r_0} z' J_0(z')\,dz' \\ &= \frac{2\pi}{(k\sin\theta)^2} z_0' J_1(z_0') \\ &= 2\pi r_0^2 \frac{J_1(z_0')}{z_0'} \end{aligned} \tag{12}$$

By using formula (12), formula (11) becomes

$$P_A = -w^2 \frac{\rho}{2} \sum_{r=1}^{\infty} \left\{ \frac{u_i \left(\sum^{k} u_m r_0^2 \Phi_m\right)}{a_r (j\omega - p_r)} + \frac{u_i^* \left(\sum^{k} u_m^* r_0^2 \Phi_m\right)}{a_r^* (j\omega - p_r^*)} \right\} \exp(-jkl) \cdot F_i / l \tag{13}$$

where, $\Phi = 2 \frac{J_1(z_0')}{z_0'}$

$$P_A / F_i = -w^2 \frac{\rho}{2} \exp(-jkl) \sum_{r=1}^{\infty} \left\{ \frac{u_i \left(\sum^{k} u_m r_0^2 \Phi_m\right)}{a_r (j\omega - p_r)} + \frac{u_i^* \left(\sum^{k} u_m^* r_0^2 \Phi_m\right)}{a_r^* (j\omega - p_r^*)} \right\} \tag{14}$$

Suppose that every diameter of pistons is the same value

$$P_A / F_i = -w^2 \frac{\rho}{2} \exp(-jkl) \sum_{r=1}^{\infty} \left\{ \frac{u_i \left(\sum^{k} u_m\right)}{b_r (j\omega - p_r)} + \frac{u_i^* \left(\sum^{k} u_m^*\right)}{b_r^* (j\omega - p_r^*)} \right\} \tag{15}$$

When the acoustic pressure is measured with shifted the retarded time (1/c),

$$P_A / F_i = -w^2 \sum_{r=1}^{\infty} \left\{ \frac{u_i u_A}{c_r (j\omega - p_r)} + \frac{u_i^* u_A^*}{c_r^* (j\omega - p_r^*)} \right\} \tag{16}$$

Where, $u_A = \sum_{m=1}^{k} u_m$

$$c_r = \frac{2 a_r l}{\rho r_0^2 \Phi}$$

Formula (16) is a frequency response function which is the ratio of an input force to an acoustic pressure with shifted a retarded time (1/c).

2.2.2 NEAR FIELD MODEL

In the near field model , the conditions (R>>d) as in the far field model are not required , therefore this model is more practical than the far field model.

Suppose that the piston surfaces are very small , formula (8) becomes

$$P_A / F_i = -w^2 \sum_{r=1}^{n} \left\{ \frac{u_i u_A}{\frac{\pi}{\rho} a_r (j\omega - p_r)} + \frac{u_i^* u_A'}{\frac{\pi}{\rho} a_r^* (j\omega - p_r^*)} \right\} \qquad (17)$$

where , $u_A = \sum_{m=1}^{L} u_m \cdot \Delta S_m \exp(-jkR)/R$

$u_A' = \sum_{m=1}^{L} u_m^* \cdot \Delta S_m \exp(-jkR)/R$

Formula (17) expresses a frequency response function in the near field. Continuous systems have an infinite number of degrees of freedom but , only a finite number of modes can be used to describe the dynamic characteristics of a system . The theoretical number of degrees of freedom can be reduced by using a finite frequency range of interest . Therefore, the frequency response can be broken up into three parts $(0, f_1 : f_1, f_2 : f_2, \infty)$. In this case Formula (17) can be expressed as follows.

$$P_A / F_i = Y_{Ai} - w^2 \sum_{r=1}^{N} \left\{ \frac{u_i u_A}{a_r (j\omega - p_r)} + \frac{u_i^* u_A'}{a_r^* (j\omega - p_r^*)} \right\} - w^2 \cdot Z_{Ai} \qquad (18)$$

A example of a frequency response is illustrated in Figure 5.

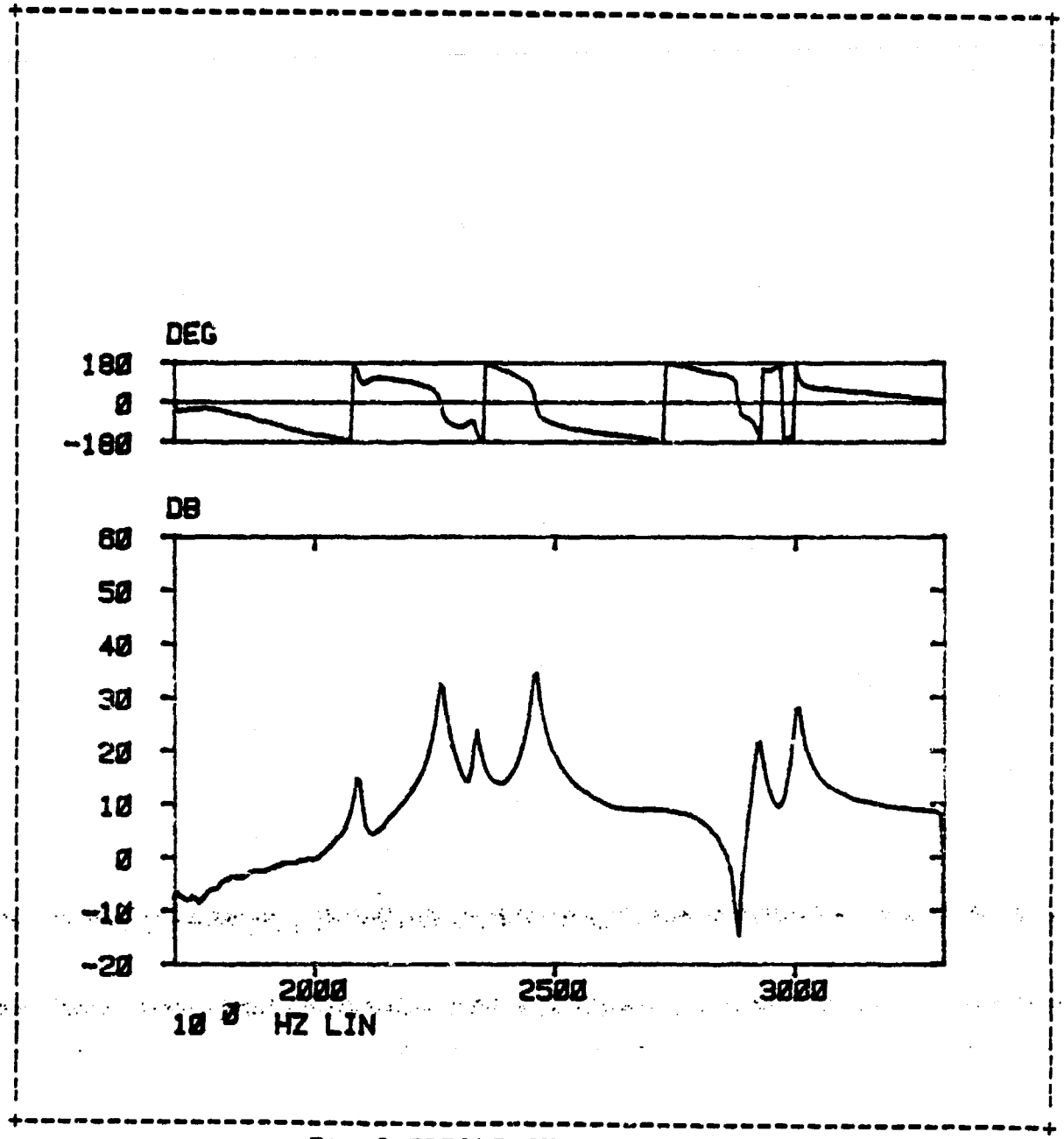

Fig.5 FREQUENCY RESPONSE FUNCTION

ESTIMATION TECHNIQUE	CHAPTER 3

As a frequency response function in the near field involves that in the far field and is more practical , in this chapter a estimation technique of the modal parameters will be developed for the near field model.

3.1 FREQUENCY/DAMPING ESTIMATION

In this section some techniques for estimating frequencues and dampings will be shown. But technique (1) through (3) are applicable only for cases where the system is lightly damped or the modes are well separated.

(1) Suppose that the difference of the two frequencies where the value of the magnitude of the frequency response becomes 1/a of the peak is Δw ,

$$\xi_r = \Delta\omega / 2\omega_r \sqrt{a^2 - 1} \qquad (19)$$

(2) Suppose that the difference of the two frequencies where the value of the quadrature response becomes 1/a of the peak is Δw ,

$$\xi_r = \Delta\omega / 2\omega_r \sqrt{a - 1} \qquad (20)$$

(3) The damping factor can be obtained by the variation of the phase angle around the resonance, that is

$$\xi_r = 1 / \{\omega_r (\partial\phi / \partial\omega)_r\} \qquad (21)$$

(4) The frequencies and dampings can be estimated as global values by an unit impulse response and a least square sense . Now the unit impulse response can be obtained by a Fourier transform of Formula (17) as

follows ,

$$h_{Ai}(t) = \sum_{r=1}^{\infty}\left\{\sum_{m=1}^{L}\frac{\Delta S_m}{R_m}\cdot\frac{u_i u_m}{a_r}\cdot e^{p_r(t-\frac{R_m}{c})} + \sum_{m=1}^{L}\frac{\Delta S_m}{R_m}\cdot\frac{u_i^* u_m^*}{a_r^*}\cdot e^{p_r^*(t-\frac{R_m}{c})}\right\}$$

$$= \sum_{r=1}^{\infty}\left\{\sum_{m=1}^{L}\frac{\Delta S_m}{R_m}\cdot\frac{u_i u_m}{a_r} e^{-\frac{p_r R_m}{c}} e^{p_r t} + \sum_{m=1}^{L}\frac{\Delta S_m}{R_m}\cdot\frac{u_i^* u_m^*}{a_r^*}\cdot e^{-\frac{p_r^* R_m}{c}}\cdot e^{p_r^* t}\right\}$$

$$= \sum_{r=1}^{\infty}\left\{A_{Ai} e^{p_r t} + A_{Ai}^* e^{p_r^* t}\right\} \qquad (22)$$

Formula (22) is the same expression as the unit impulse response of the vibration , so the same procedure as that of the vibration can be used to estimate the eigenvalues . For details see reference [4].

3.2 MODAL VECTOR ESTIMATION

The frequencies and dampings can be obtained by the technique discussed in the previous section . Therefore , modal vectors estimation technique will be developed using these parameters in this section .

A frequency response function in the near field is

$$P_A / F_i = Y_{Ai} = w^2 \sum_{r=1}^{N}\left\{\frac{u_i u_A}{a_r(j\omega - p_r)} + \frac{u_i^* u_A^*}{a_r^*(j\omega - p_r^*)}\right\} - w^2 \cdot Z_{Ai} . \qquad (18)$$

This equation will be used to estimate the modal vector ,but this is difficult to solve because the numerators are not constant and it is supposed to be a big matrix problem , so it is not practical to directly use this equation . Now in order to solve this problem a iteration procedure will be used (Figure 6) .

First of all, the numerators are assumed to be constant complex ,that is

$$P_A / F_i = Y_{Ai} = w^2 \sum_{r=1}^{N}\left\{\frac{A_{ir} + jB_{ir}}{j\omega - p_r} + \frac{A_{ir} - jB_{ir}}{j\omega - p_r^*}\right\} - w^2 \cdot Z_{Ai} \qquad (23)$$

Equation (23) will be used to solve the first approximaion of modal vectors. That is , A +jB is estimated from Formula (23) ,then by the relation of Formula (18) and (23), the following N equations can be obtained .

$$u_i \cdot \left\{\sum_{m=1}^{L} u_m S_m \cdot \exp(-jkR_m)/R_m\right\} / a_r = A_{ir} + jB_{ir} \qquad (24)$$
$$(i = 1, N)$$

Equations (24) can be solved as follows,

$$u_i/\sqrt{a_r} = (A_{ir}+jB_{ir}) \Big/ \sqrt{\sum_{m=1}^{M} (A_m+jB_m)\cdot \exp(-jkR_m)\ S_m/R_m} \qquad (i=1,N) \qquad (25)$$

Solutions (25) are the first approximation of modal vectors.

(25) are instituted into $u_A/\sqrt{a_r}$, $u_A'/\sqrt{a_r}$ (see (17) in page 9) of equation (18) ,then from (18) $u_i/\sqrt{a_r}$ can be estimated again. Next , these solutions are instituted into the same terms of (18) as the above again and $u_i/\sqrt{a_r}$ are estimated again.

The above procedures are repeated until the change of the solutions will be enough small .

In order to estimate the modal vectors from equation (18) and (23) a least square method will be used. Let G represent the experimentally determined frequency response function , and H represent the mathematical model of formula (18),(23)

$$\left(\frac{P_A}{F_i}\right)_{EXP} = G(f) \qquad f=f_1, f_2, f_3, \ldots, f_m \qquad (26)$$

$$\left(\frac{P_A}{F_i}\right)_{model} = H(f,\gamma) = H(f,\gamma_1,\gamma_2,\ldots,\gamma_M) \qquad f=f_1, f_2, \ldots, f_m \qquad (27)$$

where γ is modal vector

The error in the fit at frequency f_k is

$$E_k(\gamma) = G(f_k) - H(f_k,\gamma) \qquad (28)$$

By minimizing the error term E_t the modal vector can be determined. That is

$$E_t = \sum_{k=1}^{m} E_k(\gamma)\cdot E_k^*(\gamma) = \sum_{k=1}^{m} |E_k(\gamma)|^2 \qquad (29)$$

$$\frac{\partial E_t}{\partial \gamma} = \sum_{k=1}^{m} \left[E_t \frac{\partial H}{\partial \gamma_i}(f_k,\gamma) + E_t^* \frac{\partial H^*}{\partial \gamma_i}(f_k,\gamma)\right] = 0 \qquad (30)$$

the number of equations (30) is 2M+2 , so the 2M+2 unknowns(modal vector) can be solved from equations (30). See Appendix A.

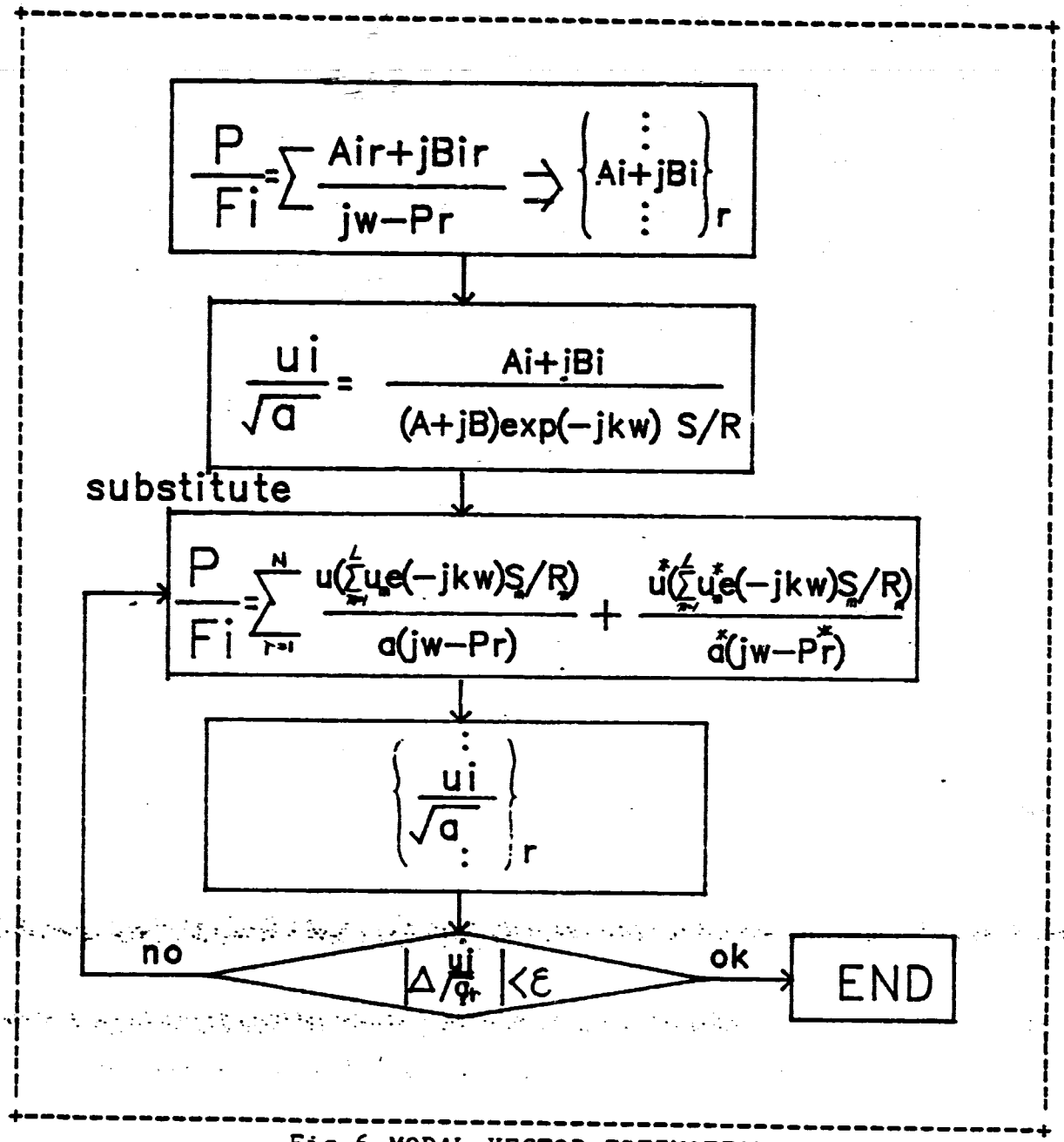

Fig.6 MODAL VECTOR ESTIMATION FLOW

3.3 MODAL VECTOR SCALING

By the iteration technique u / ar (i=1,N,r=1,M) can be estimated The denominator of this is a scaling factor of a modal vector.

Suppose that a scaling factor is R+jI ,

$$a_r = (R+jI) \tag{31}$$

For the case of proportional damping ,

$$a_r = j4\pi m_r w_{ar}/S \tag{32}$$

Therefore , $$m_r = |R+jI|S/4\pi w_{ar} \tag{33}$$

Here a modal mass can be obtained.

RESULT OF ANALYSIS AND EXPERIMENT	CHAPTER 4

To check the effectiveness of this technique developed in the previous chapter, two examples were tested in the anechoic chamber. The first example involves the turbine blade and the second example is T-plate. The results will be shown below.

4.1 TURBINE BLADE

The turbine blade structure is schematically shown in Figure 7. The microphone was set at 10 centimeters away from the structure and each point on the structure was impacted by a small hammer. As this structure is small, the characteristics would change under the condition with an accelrometer. But, to verify the results the vibration and the acoustic test were performed with the accelrometer.

The mode shapes of the both test are shown in Figure 8 through Figure 14. The Table 1. shows Frequencies, Dampings and MAC value between the acoustic and vibration.

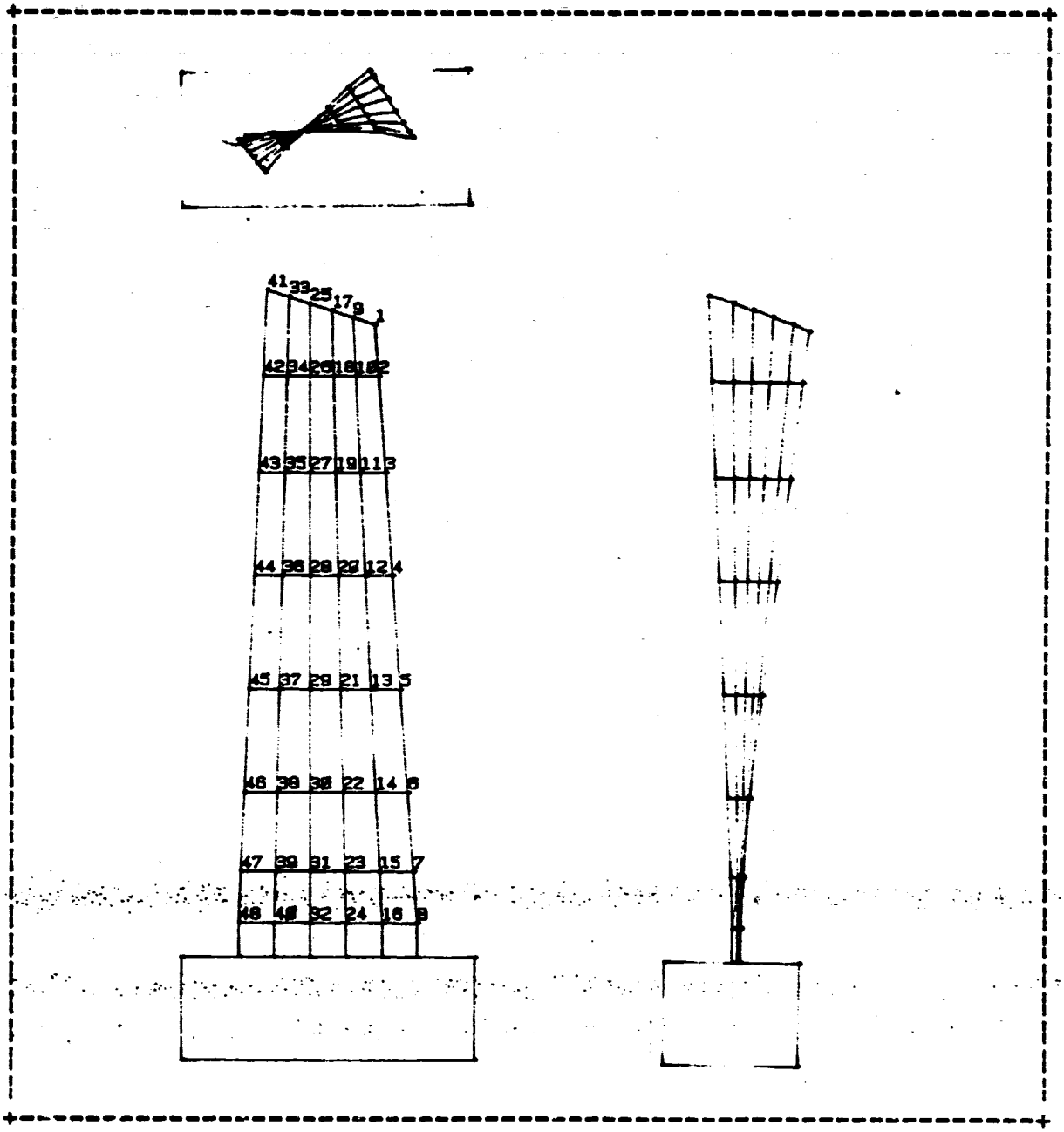

Fig. 7 TURBINE BLADE STRUCTURE

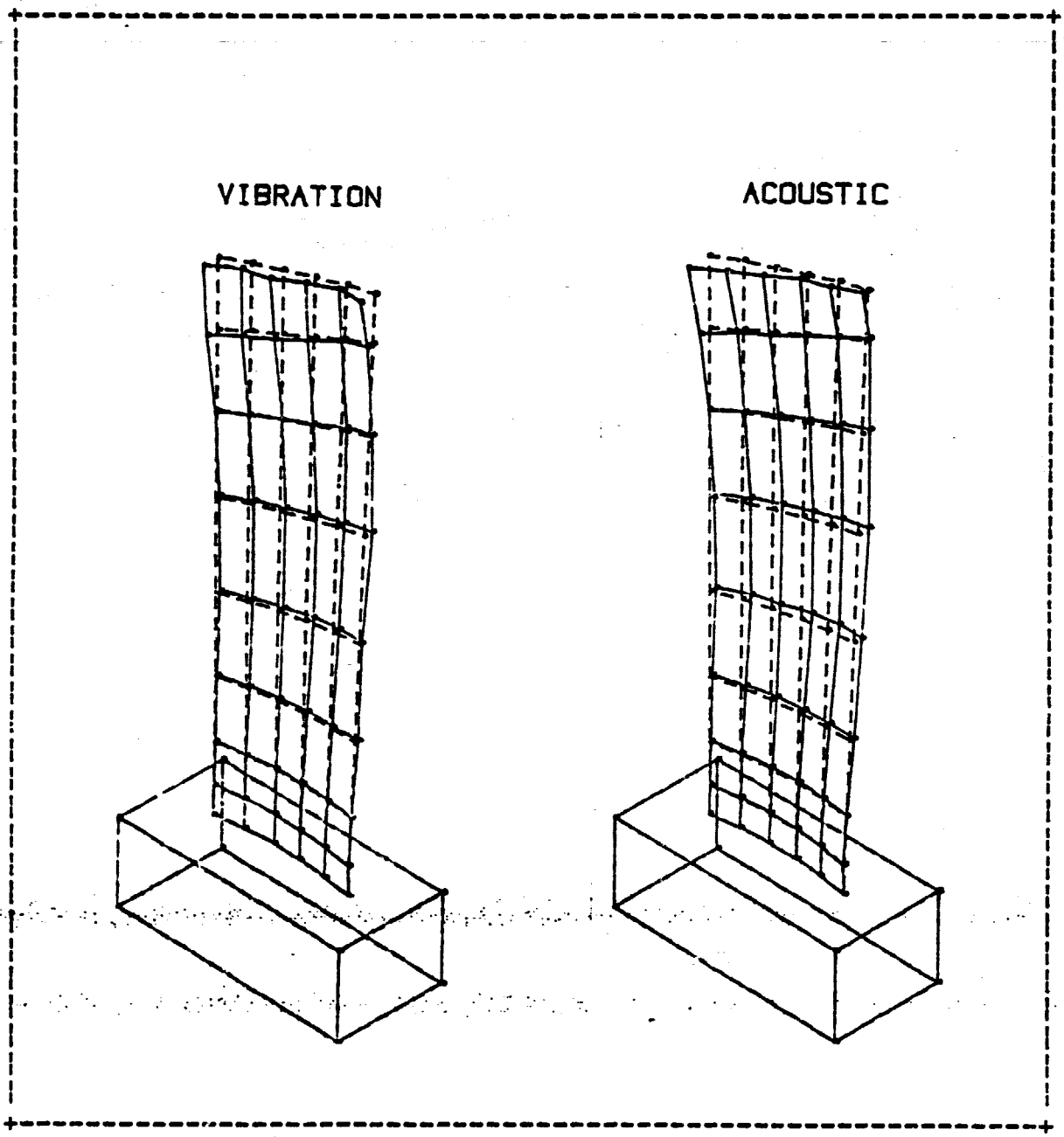

Fig. 8 MODE SHAPE 1 (TURBINE BLADE)

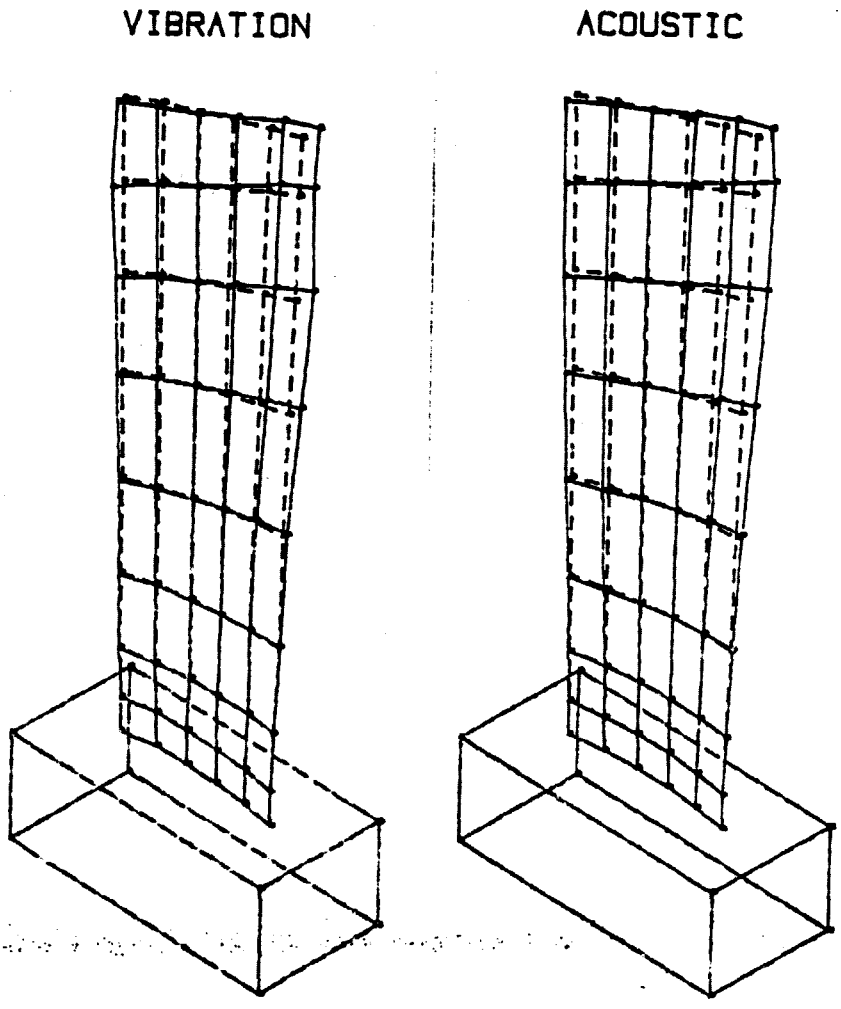

Fig. 9 MODE SHAPE 2 (TURBINE BLADE)

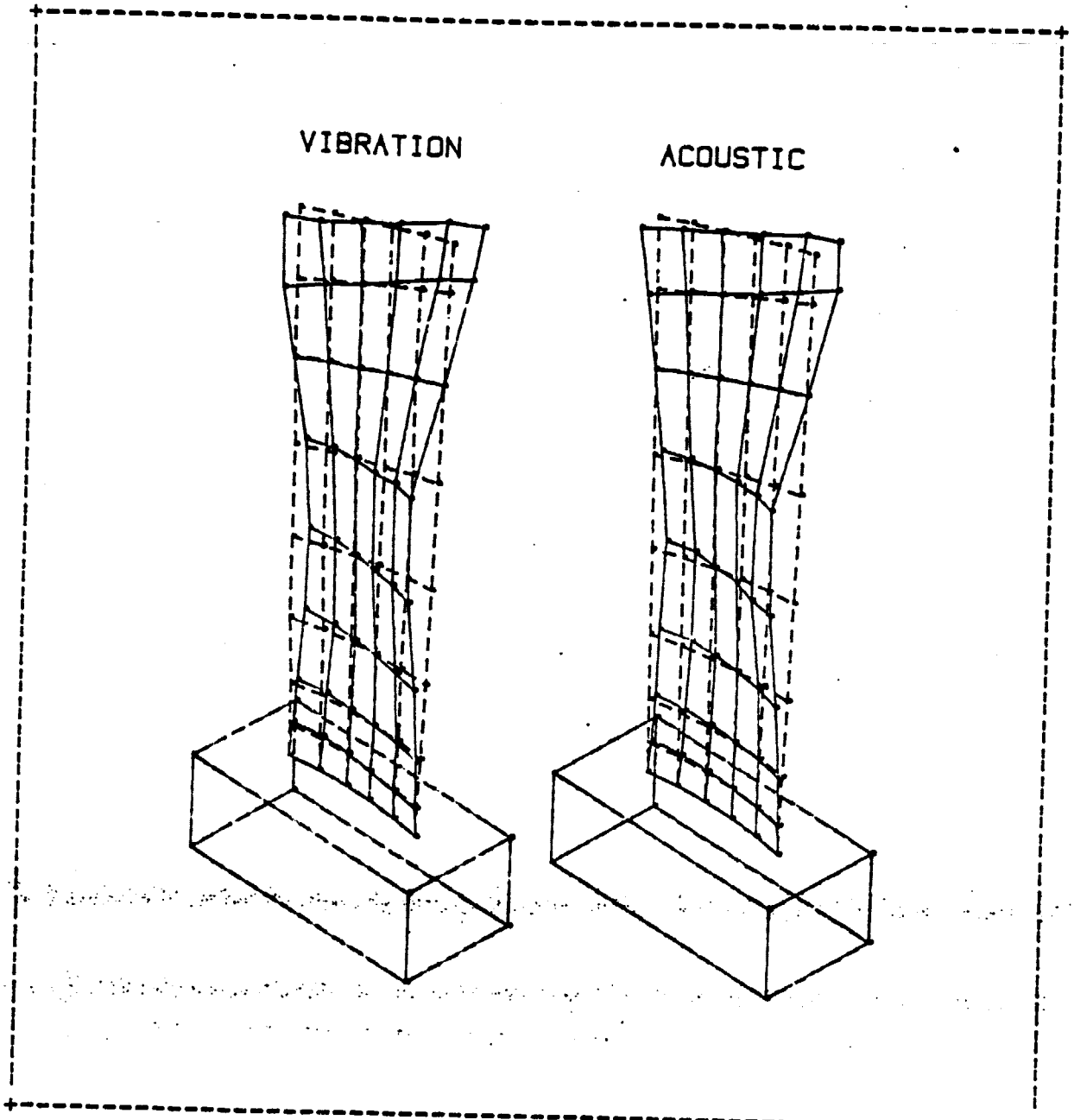

Fig .10 MODE SHAPE 3 (TURBINE BLADE)

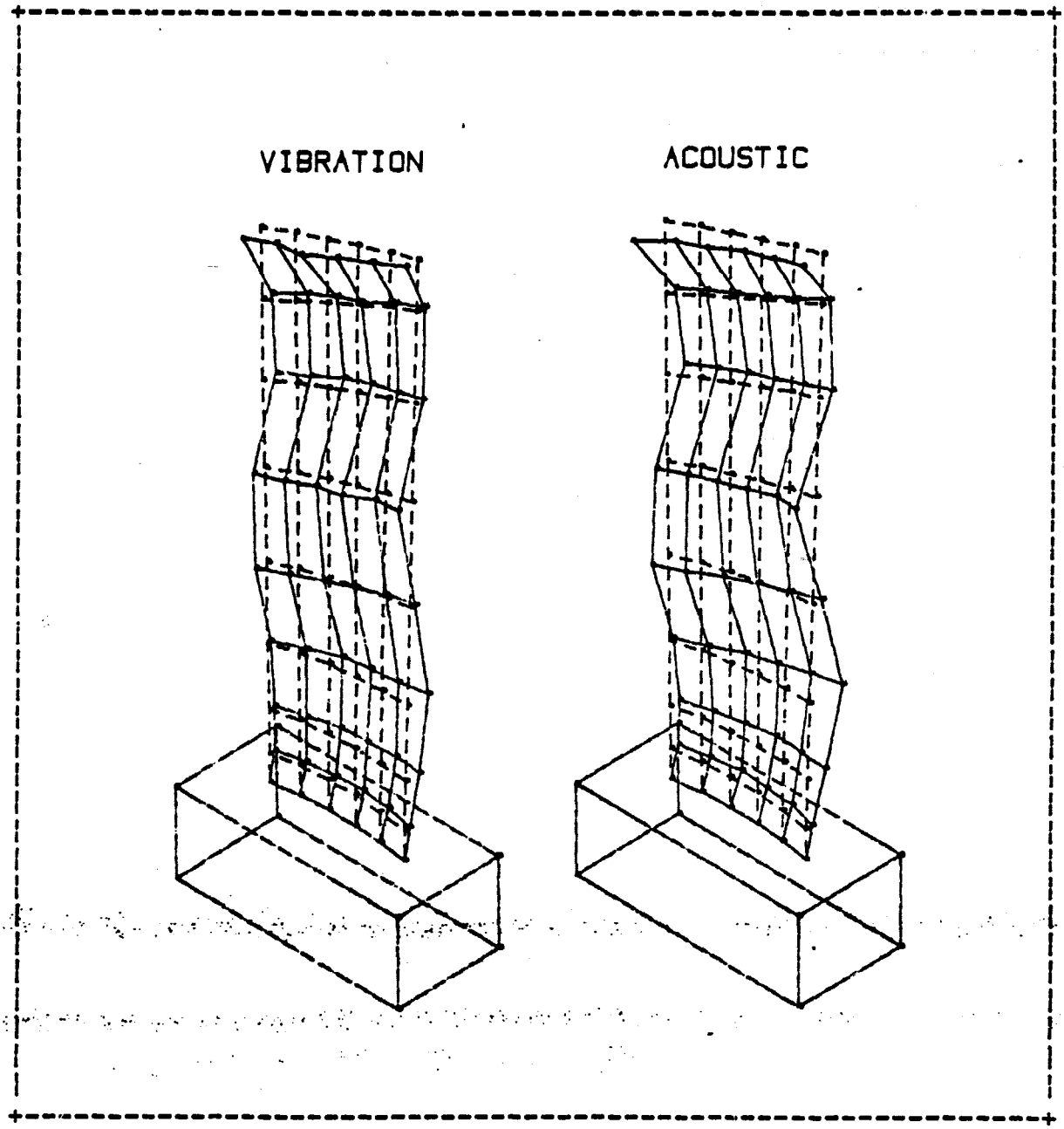

Fig. 11 MODE SHAPE 4 (TURBINE BLADE)

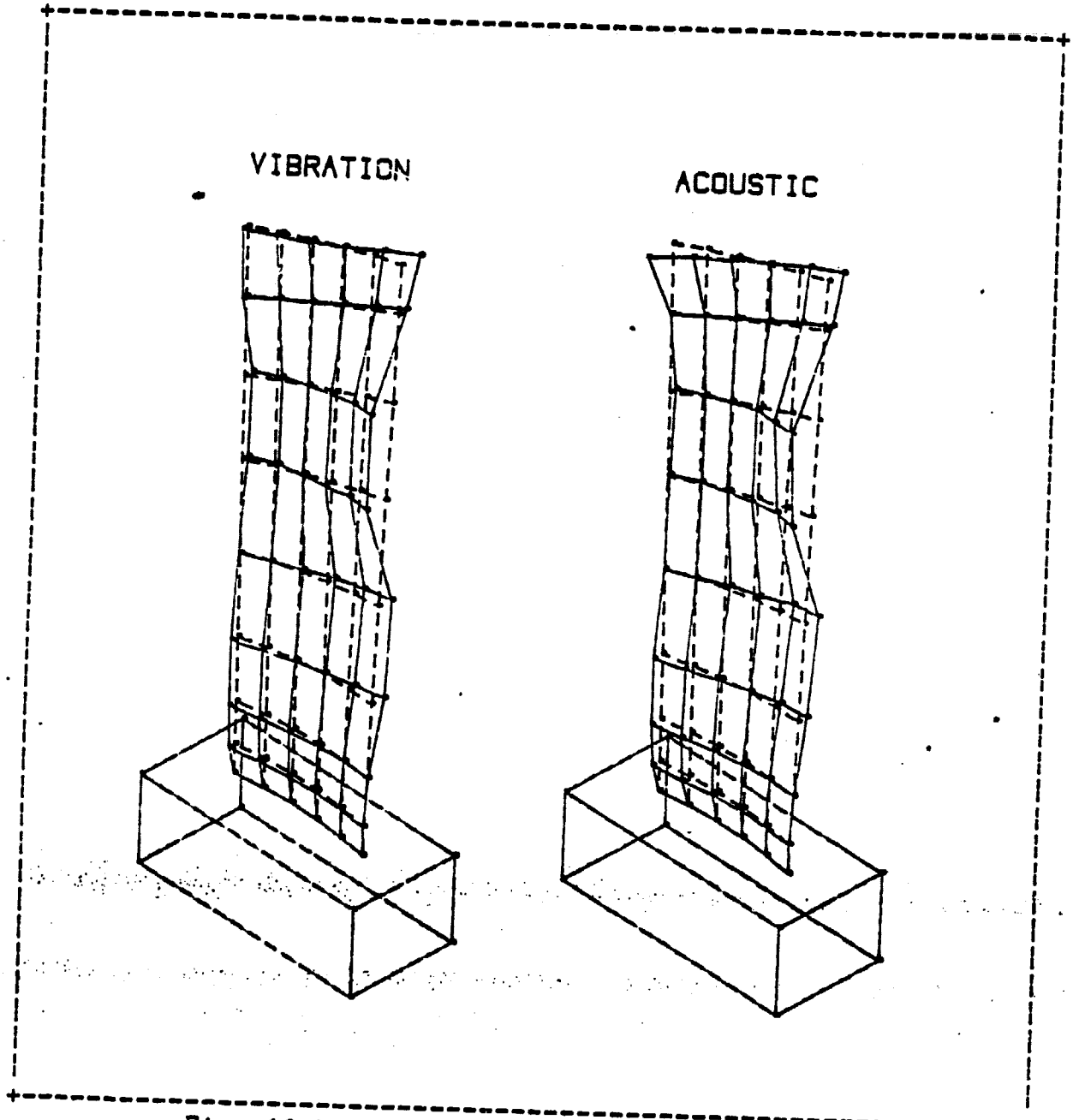

Fig. 12 MODE SHAPE 5 (TURBINE BLADE)

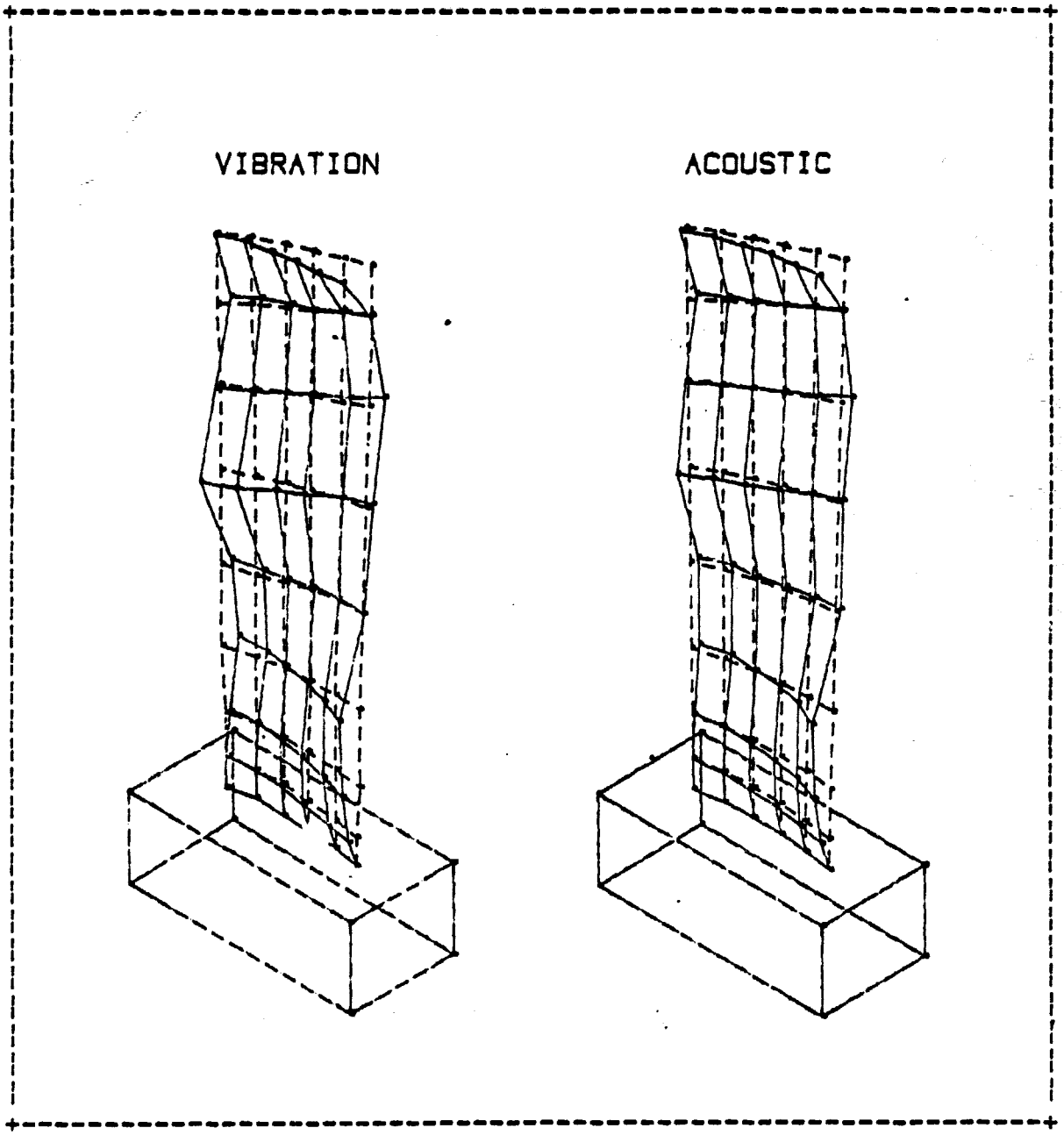

Fig. 13 MODE SHAPE 6 (TURBINE BLADE)

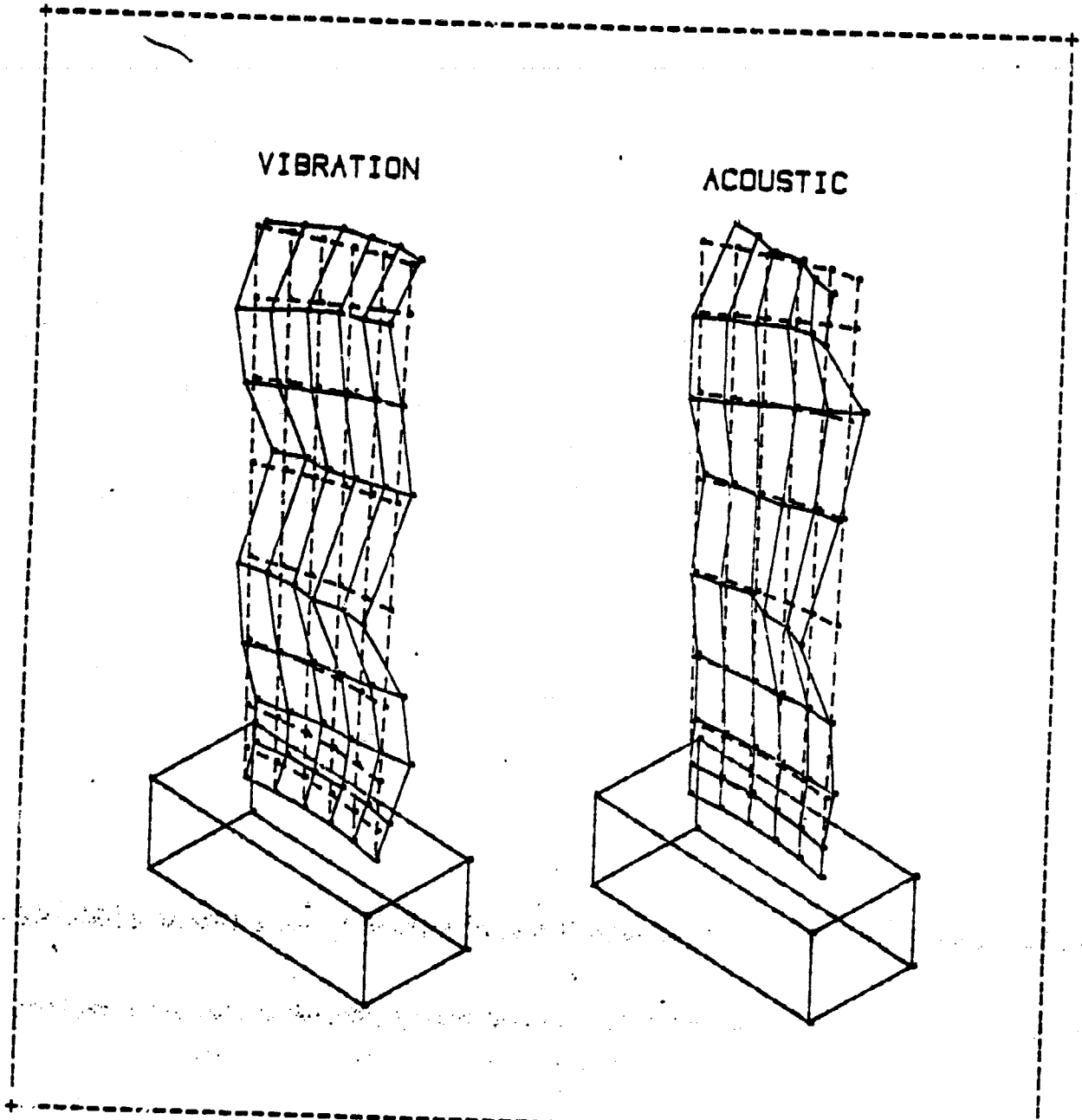

Fig. 14 MODE SHAPE 7 (TURBINE BLADE)

MODE #	FREQUENCY(Hz)		DAMPING(%)		M.A.C.
	ACO.	VIB.	ACO.	VIB.	
1	465.7	466.5	2.681	2.546	0.878
2	912.0	911.9	1.317	1.334	0.964
3	2274.6	2274.7	0.478	0.433	0.974
4	2572.7	2573.6	0.648	0.634	0.942
5	3661.1	3660.3	0.489	0.450	0.915
6	3952.0	3952.4	0.507	0.477	0.932
7	4199.5	4182.1	1.698	1.434	

Table 1 FREQUENCY,DAMPING AND M.A.C.

4.2 T-PLATE

The test configuration is illustrated in Figure 15, Figure 16.

* It was tested at a microphone position 1 as in Figure 15.
* The number of points is 96 as in Figure 16.
* The microphone used is B&K one inch microphone and the analyser is HP-5423A .
* The frequency range is 1706.25Hz to 3306.25Hz.

In order to compare the results it was also tested with an accelrometer at a point 91.

4.2.1 CONTRIBUTION OF MODE TO NOISE

As mentioned earlier this technique has merits as below.

(1) Modes which contribute much to the total noise at a certain microphone position can be directly found.
(2) It is not necessary to attach an accelrometer onto the structure.

Item(1) is shown in Figure 17. These data are a summation of frequency response functinos at all points on the structure.

In case of the vibration test this kind of data much depends on a point which an accelrometer is attached to. In this case , mode 1 does not seem to be significant mode , but by the lower data mode 1 can be recognized to be a mode which contributes much to the total noise at this microphone position.

To check the affect of the accelrometer load, the tests were performed with and without the accelrometer. The result is shown in Table 2. The significant changes in frequency can be found. This changes could be remarkable for a small structure, so this technique is also applicable for a small structure.

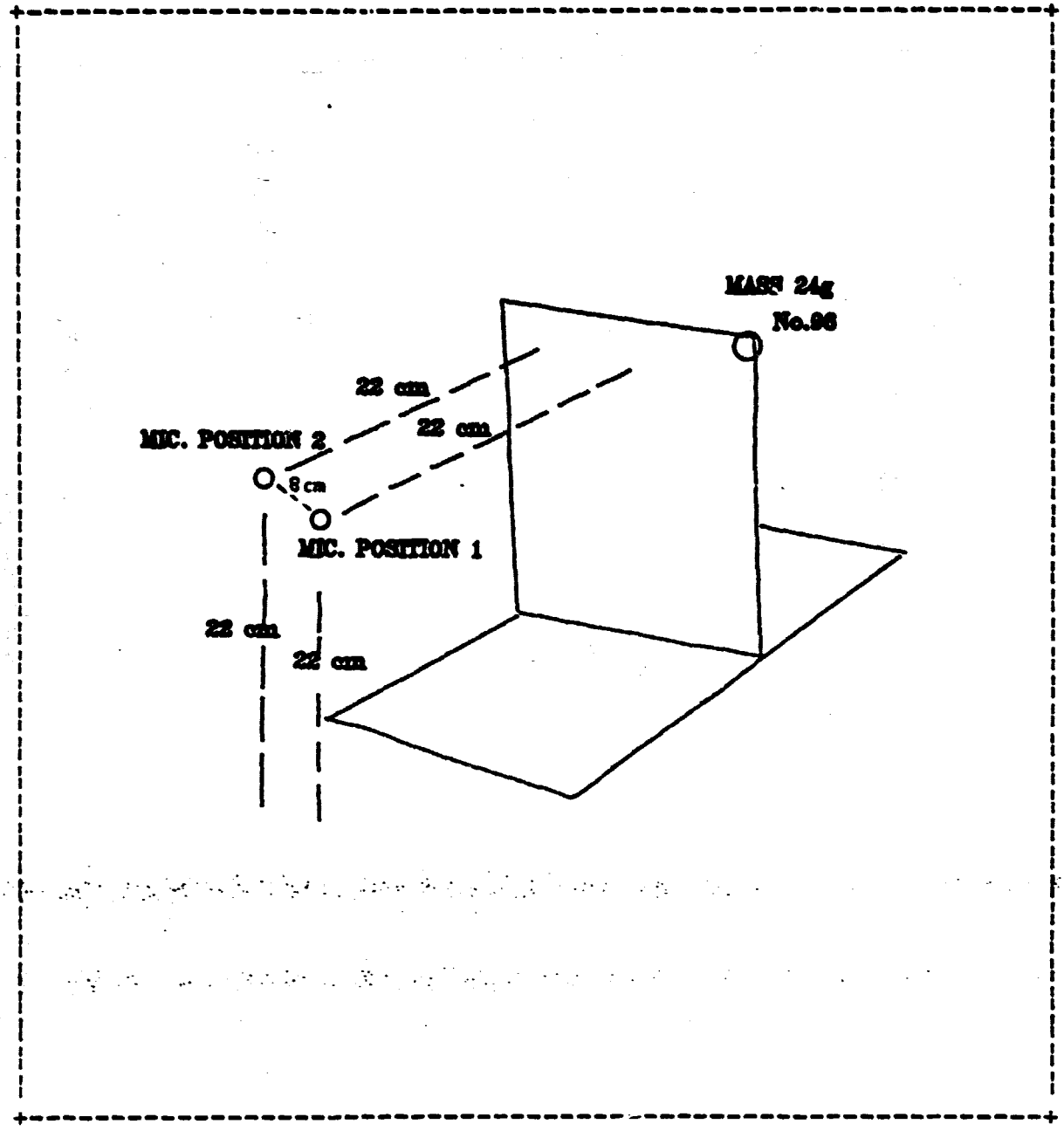

Fig.15 TEST CONFIGURATION OF T-PLATE

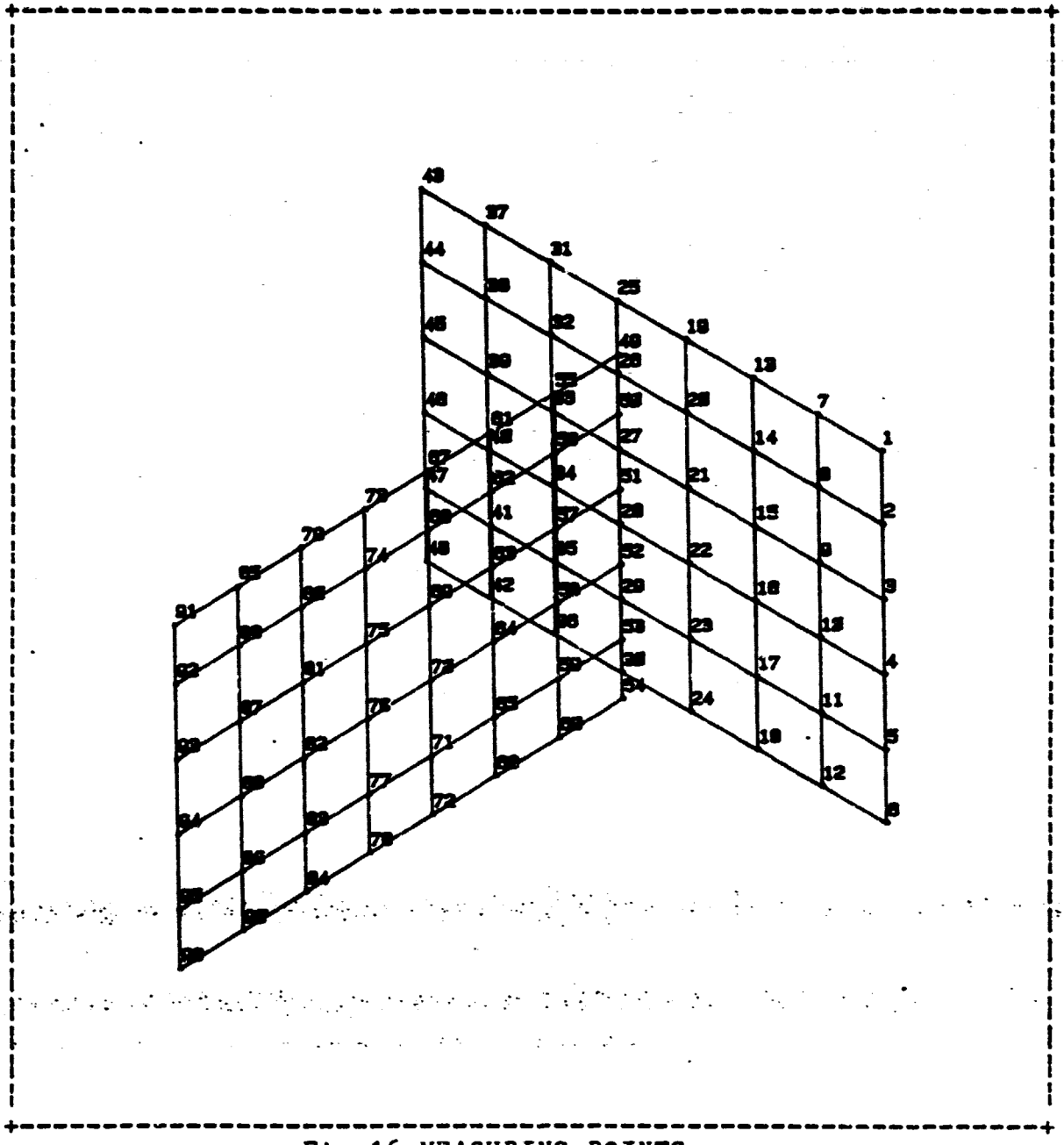

Fig.16 MEASURING POINTS

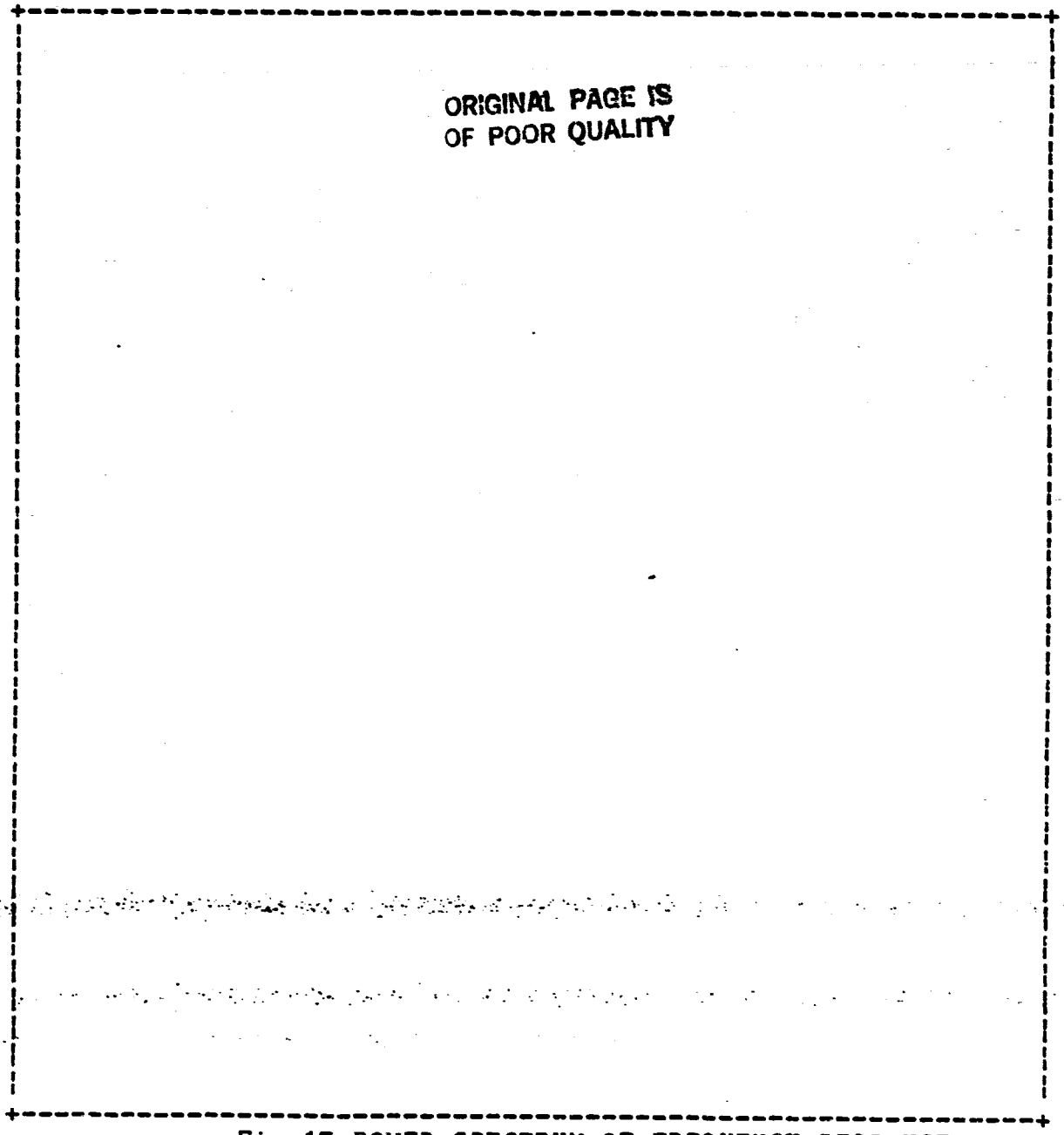

Fig.17 POWER SPECTRUM OF FREQUENCY RESPONSE

MODE #	FREQUENCY(HZ)		DAMPING(%)	
	WITHOUT	WITH	WITHOUT	WITH
1	2091.0	2087.3	0.260	0.321
2	2265.1	2260.8	0.266	0.251
3	2336.5	2336.2	0.270	0.240
4	2459.6	2422.4	0.214	0.254
5	2921.4	2912.4	0.202	0.234
6	3002.7	2980.6	0.176	0.216

Table 2 MODAL PARAMETERS WITH AND WITHOUT ACCELROMETER

4.2.2 FREQUENCY AND DAMPING

Using the least square complex exponetial algorithm discussed in the previous chapter , frequencies and dampings were estimated. The results are shown in Table 3.

MODE #	FREQUENCY(HZ)		DAMPING(%)	
	ACOUSTIC	VIBRATION	ACOUSTIC	VIBRATION
1	2086.3	2086.0	0.199	0.193
2	2260.2	2260.5	0.184	0.184
3	2334.4	2335.2	0.193	0.178
4	2420.4	2418.7	0.215	0.246
5	2910.3	2911.6	0.206	0.187
6	2978.7	2980.0	0.242	0.191

Table 3 FREQUENCIES AND DAMPINGS

4.2.3 MODAL VECTOR

In this section, the results by the technique discussed in the previous chapter ¬will be shown. Figure 18 sho-s the curve fitted data. Figure 19 to Figure 24 show the mode shape of T-plate. Table 4 shows the modal assurance criterion between the results from the acoustic and the vibration , and the modal mass.

Some modes have good correlation but some not. As this reason the followings are cosidered,

(1) As some modes were very small , it was difficult to correctly estimste so the results have some errors. This would be able to be refered to both of the acoustic and the vibration.
(2) For some modes , the acoustic radiation model used in this paper may not be applicable.

For the purpose of checking the accuracy of the results from the technique in this paper , the attempts shown in the next section were tried.

4.2.4 ACCURACY VERIFICATION

First trial was that the frequency response were predicted at the different microphone position from that where the results were esimated , by using the modal parameters. The results were shown in Figure 25 to 27 .

Next, the structure was modified by adding the mass to the point 96 as shown in Figure 15. And the frequency response were predicted at the microphone position 1 by using the modal parameters obtained by this technique. The rersults were shown in Table 5 and Figure 28 to 30 .

Fig.18 CURVE FITTED DATA (response /input)

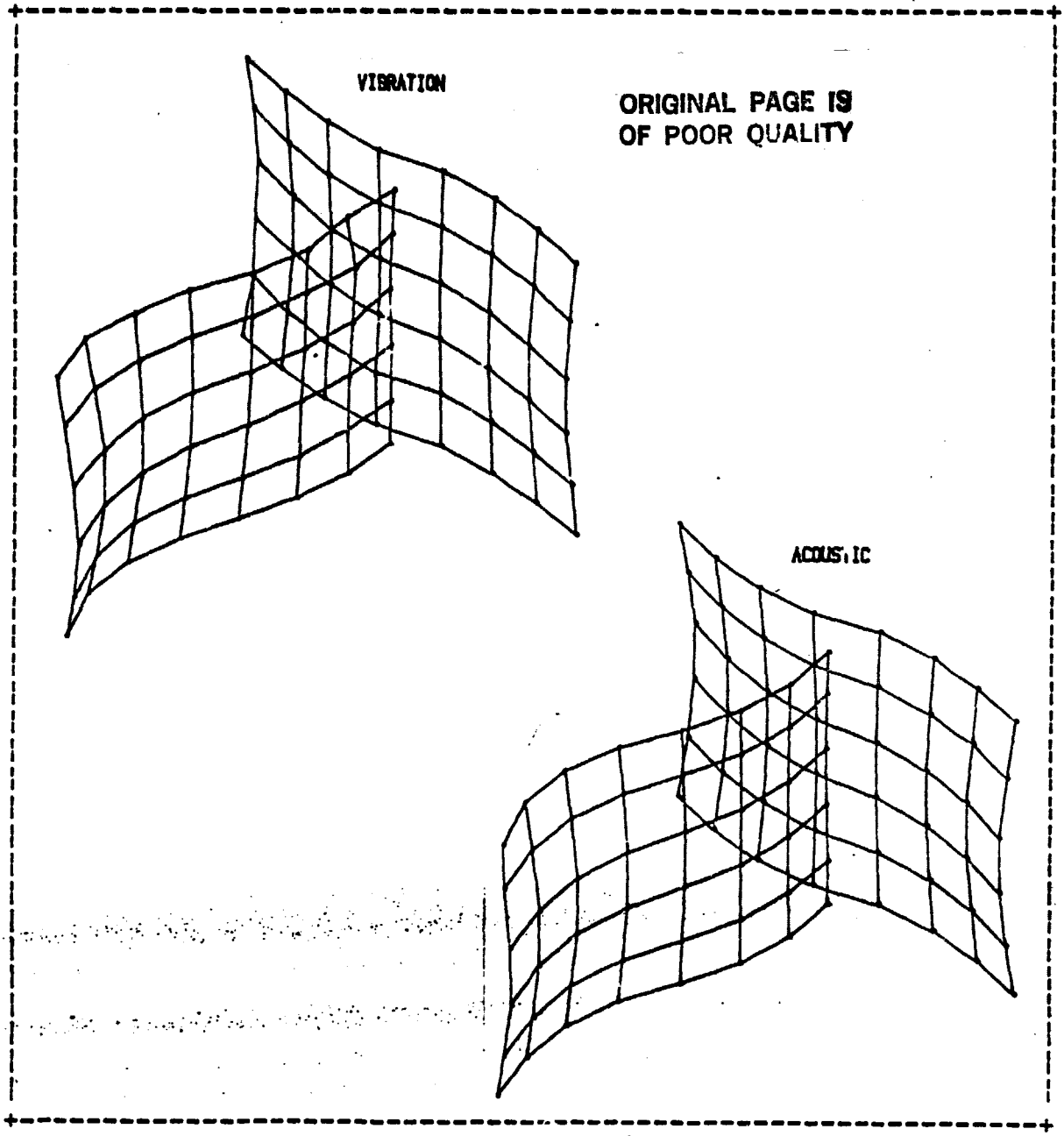

Fig.19 MODE SHAPE 1 (T-PLATE)

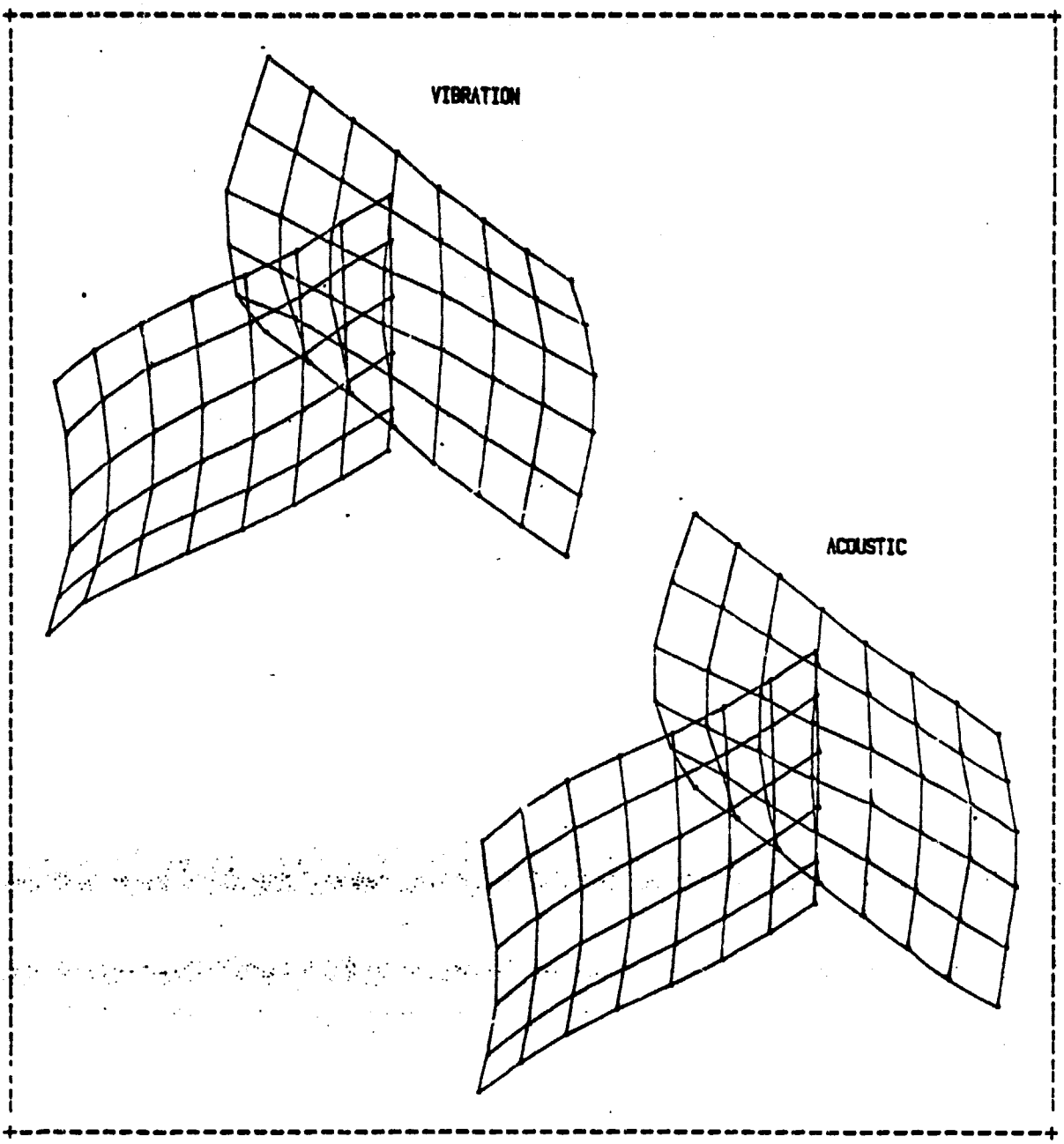

Fig.20 MODE SHAPE 2 (T-PLATE)

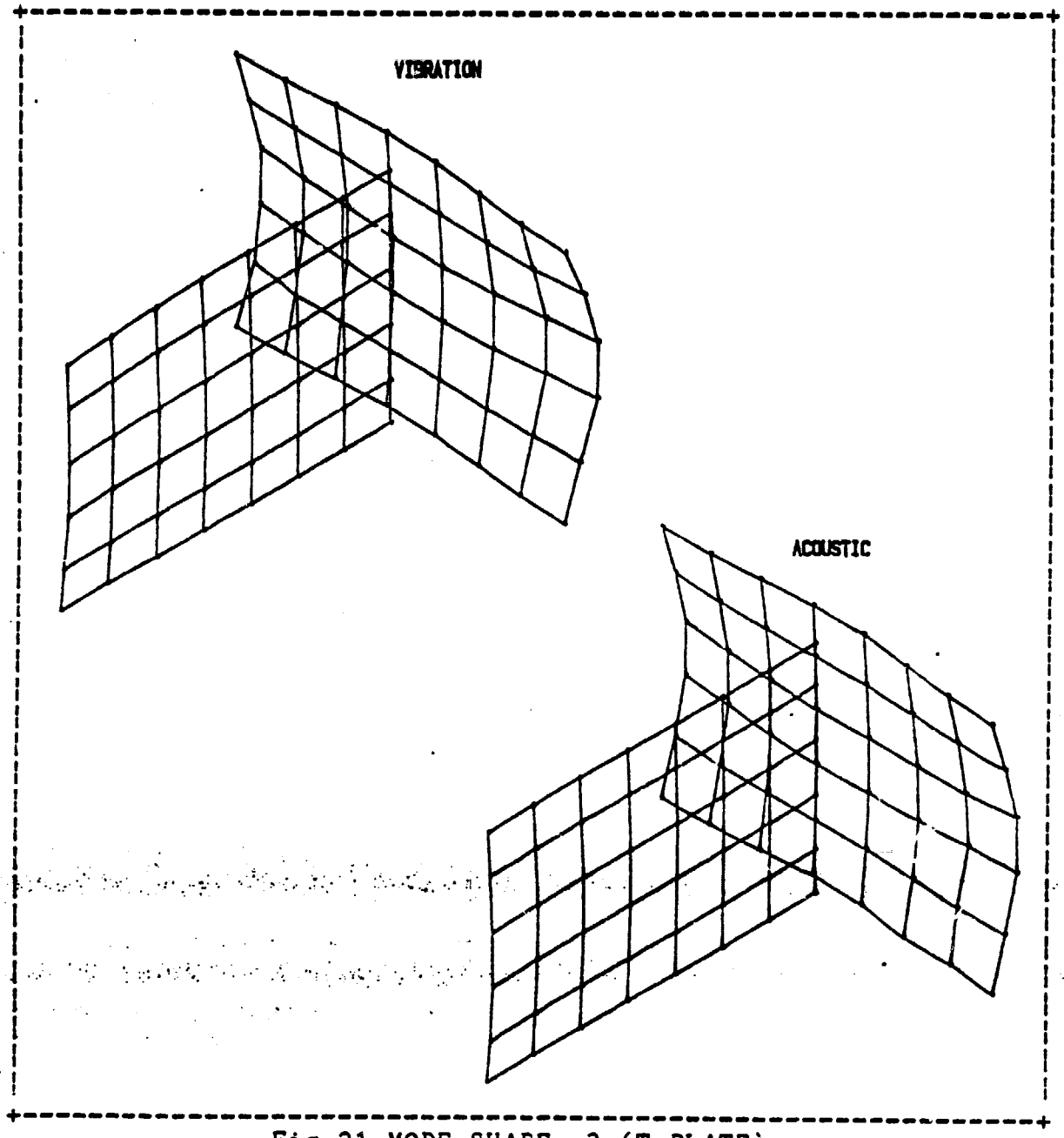

Fig.21 MODE SHAPE 3 (T-PLATE)

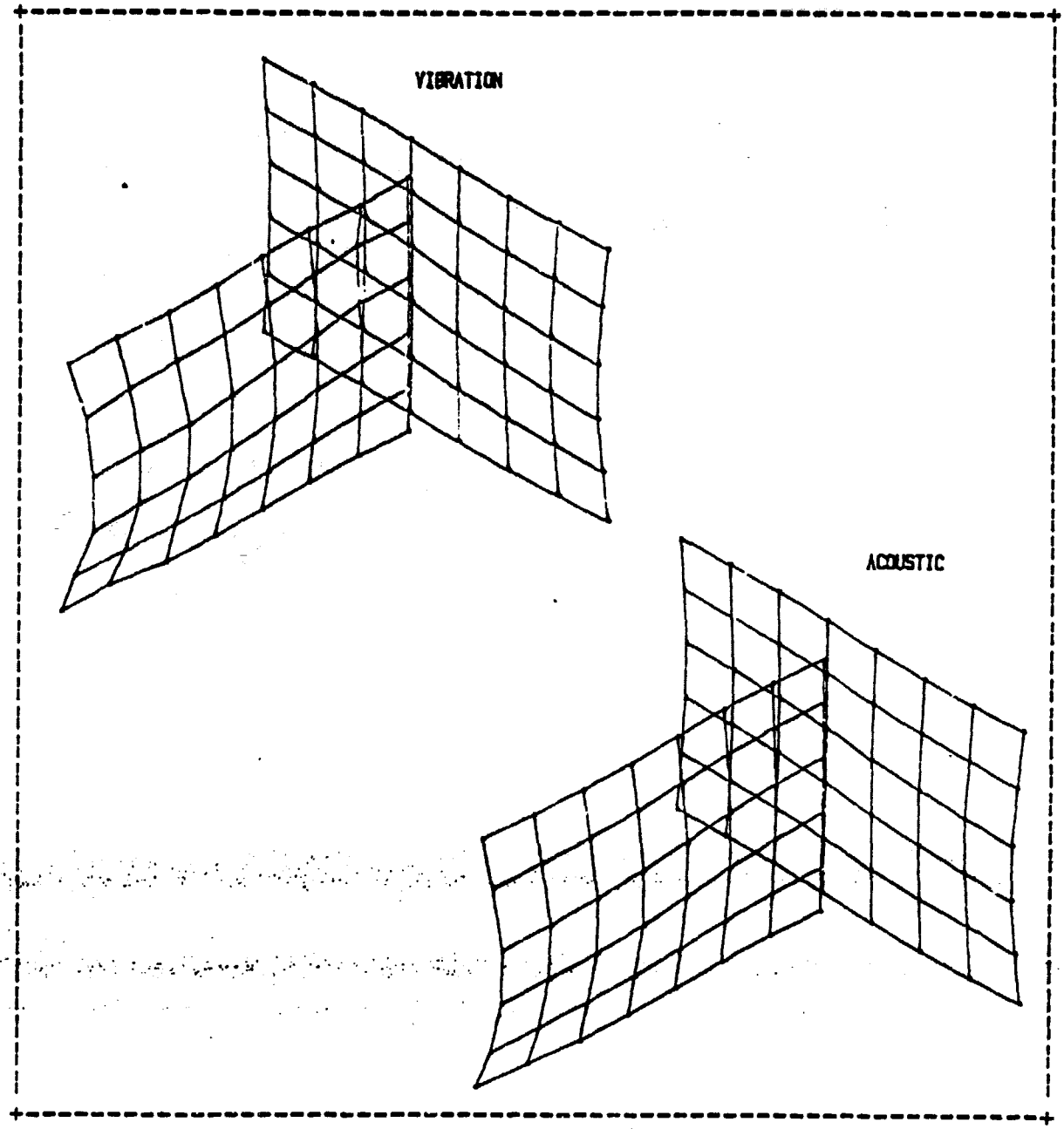

Fig.22 MODE SHAPE 4 (T-PLATE)

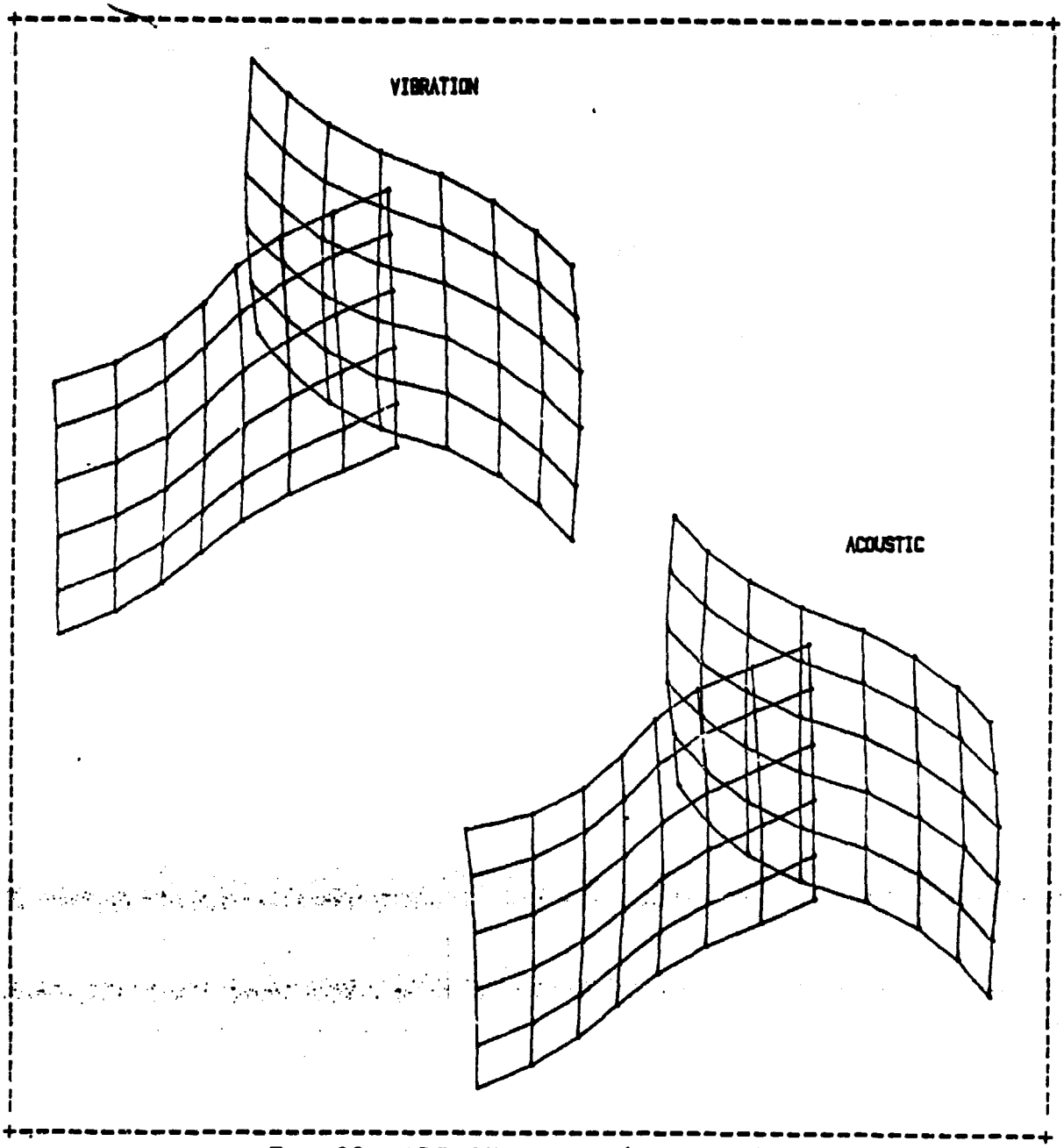

Fig.23 MODE SHAPE 5 (T-PLATE)

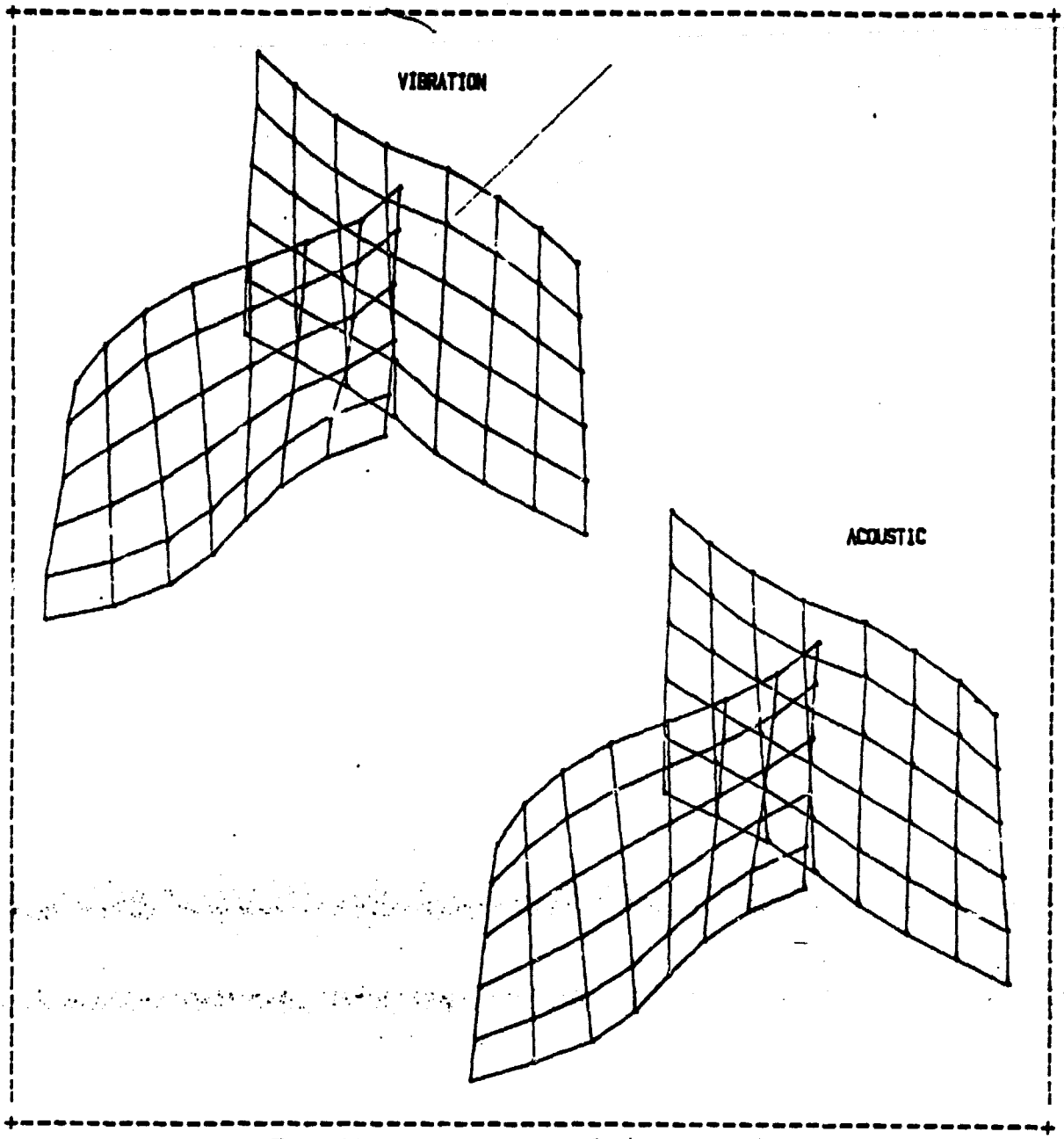

Fig.24 MODE SHAPE 6 (T-PLATE)

MODE #	MODAL MASS* (Kgm)		M.A.C.
	ACOUSTIC	VIBRATION	
1	0.151	3.140	0.782
2	0.402	0.108	0.885
3	0.204	0.206	0.924
4	0.116	0.102	0.948
5	0.151	0.111	0.941
6	0.176	0.153	0.924

* SCALING METHOD; VECTOR LENGTH UNITY

Table 4 M.A.C. AND MODAL MASS

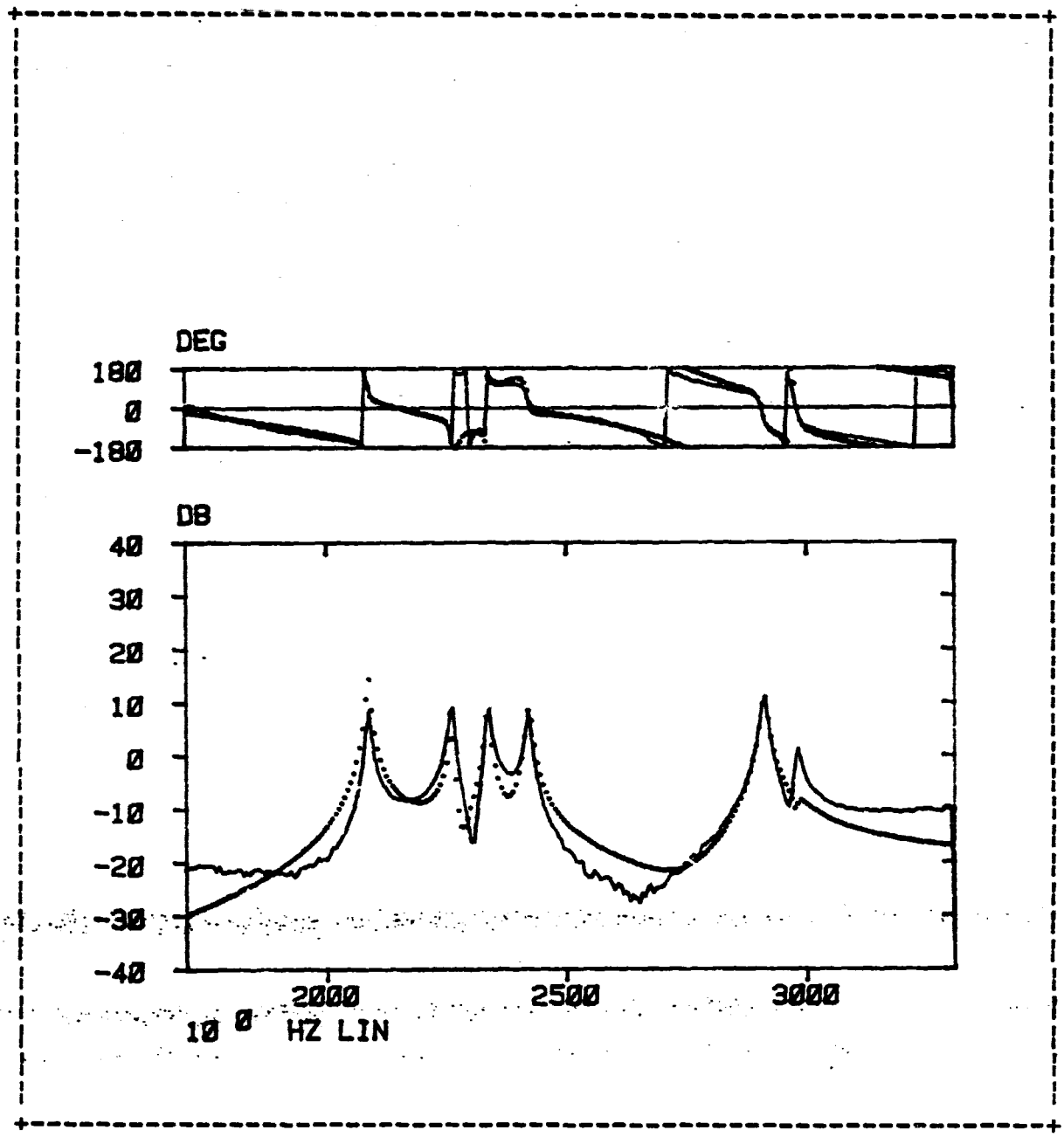

Fig.17 FREQUENCY RESPONSE (Input No.42 :Response MIC2)

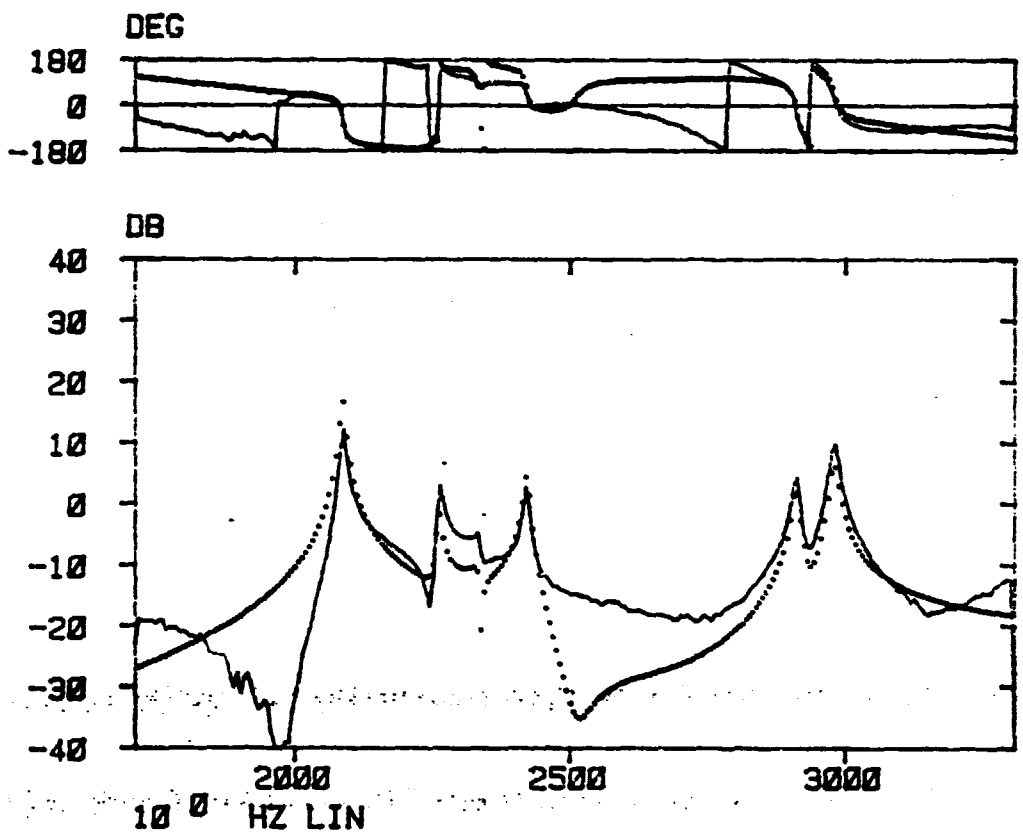

Fig.18 FREQUENCY RESPONSE (Input No.57 :Response MIC2)

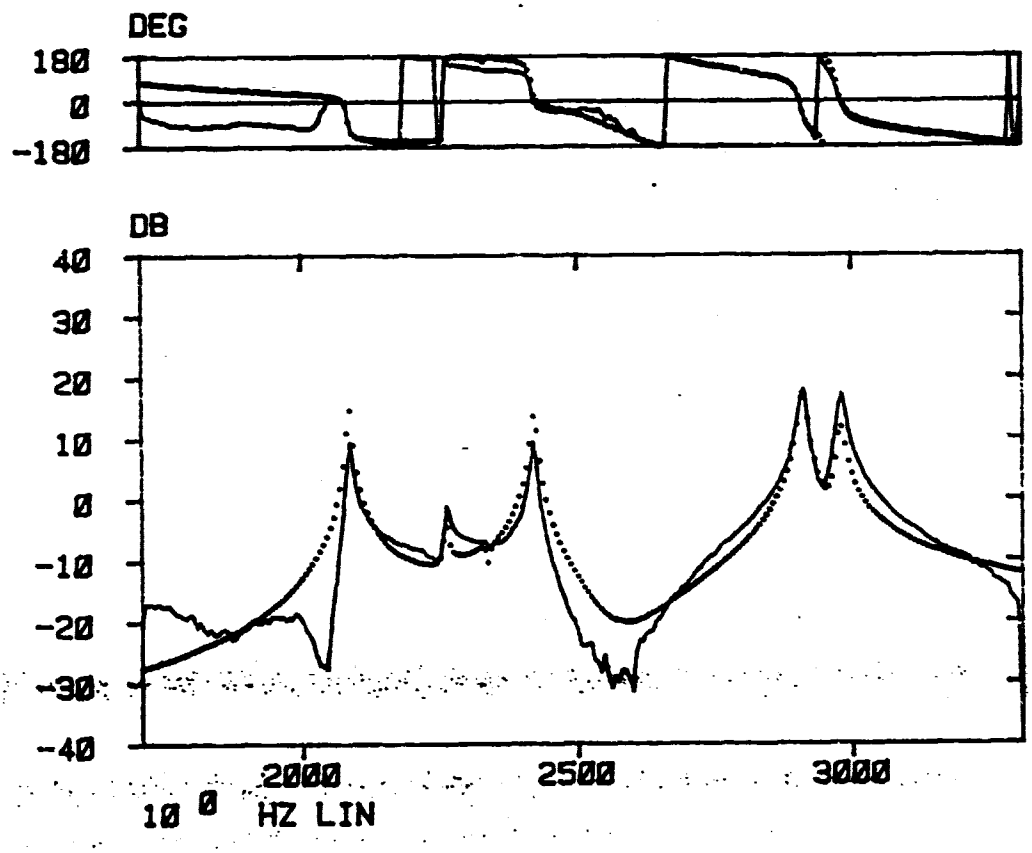

Fig.19 FREQUENCY RESPONSE (Input No. 12 :Response MIC2)

MODE #	ORIGINAL (HZ)	MODIFIED (HZ)		
		EXPER.	ANALYSIS	
			ACOUSTIC	VIBRATION
1	2086.3	2082.8	2086.0	2086.0
2	2260.2	2255.5	2259.9	2257.1
3	2334.4	2333.8	2334.0	2334.1
4	2420.4	2387.7	2387.3	2383.2
5	2910.3	2908.1	2909.6	2910.0
6	2978.7	2957.4	2967.8	2965.9

Table 5 MODIFIED FREQUENCY

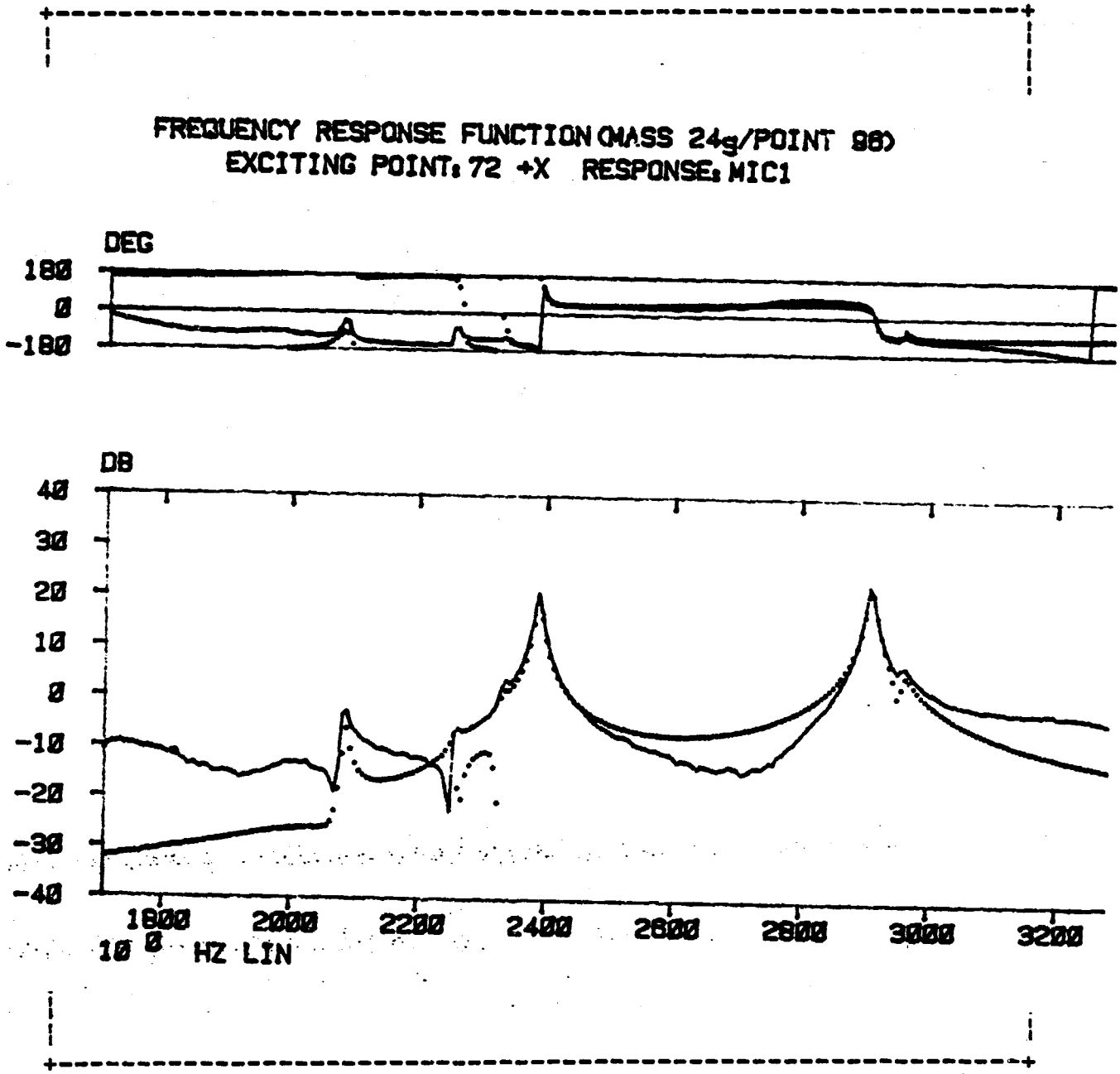

Fig.29 FREQUENCY RESPONSE (Input No.72 :Response MIC1)

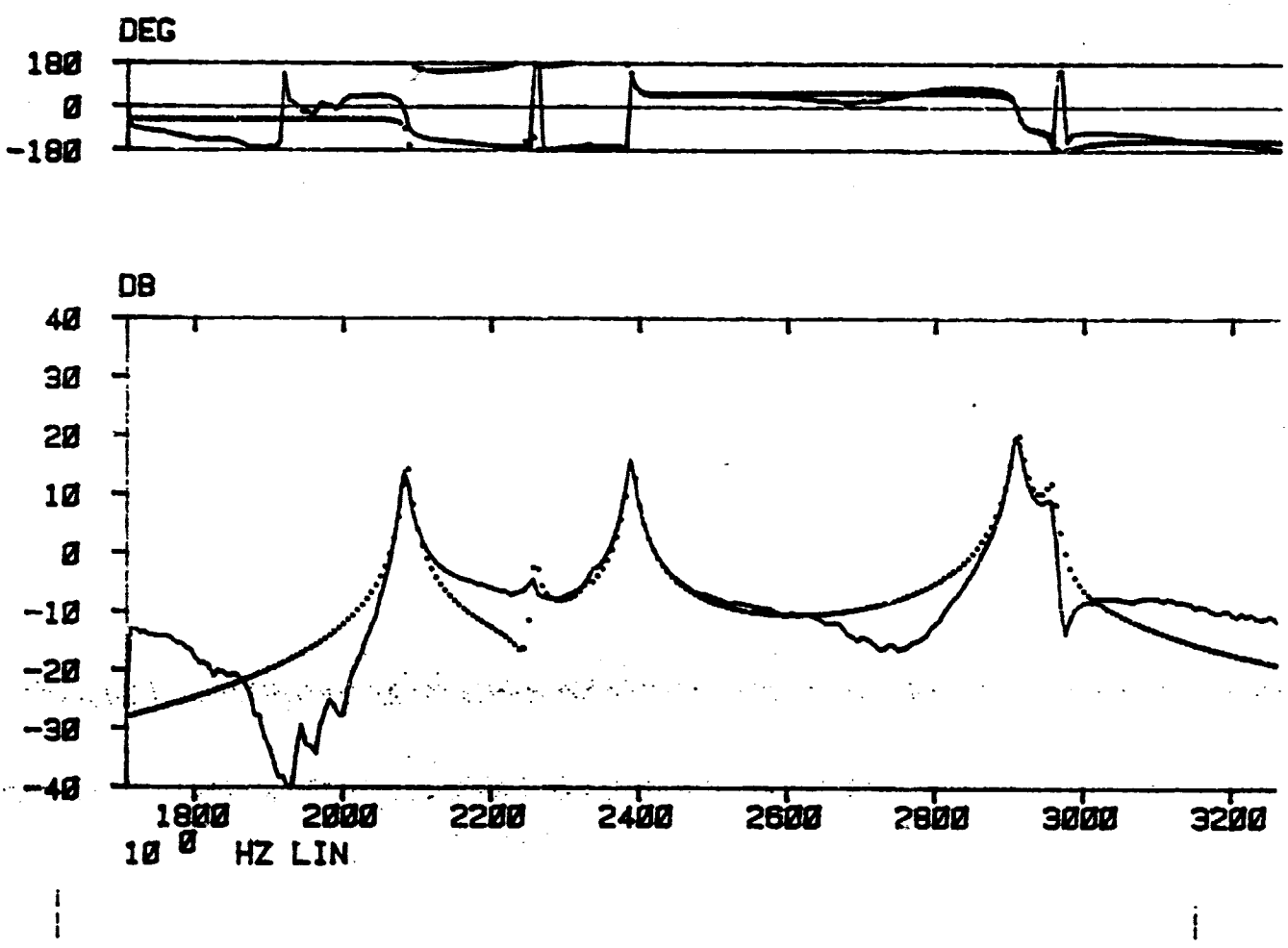

Fig.30 FREQUENCY RESPONSE (Input No.92 :Response MIC1)

ACOUSTIC MODAL PROGRAM STRUCTURE	APPENDIX B

The acoustic modal program system is based on the RTE modal program system of the University of Cincinnati , therefore it is almost the same as the modal system. But some programs have the different functions and the project file structure is different. The different programs and the project file structure will be shown below.

PROJECT FILE STRUCTURE

FIRST WORK TRACK

FIRST WORD	LAST WORD	DESCRIPTION
1	2047	COMMON
2048	2303	COMPONENT INFORMATION
2304	4351	COORDINATE INFORMATION
4352	5119	DISPLAY SEQUENCE INFORMATION
5120	6144	FREQUENCY/DAMPING INFORMATION

SECOND WORK TRACK

1	3000	RESIDUAL MASS/FLEXIBILITY
3001	6000	MODAL VECTOR ONE
6001	6144	AVAILABLE

THIRD WORK TRACK

1	3000	MODAL VECTOR TWO
3001	6000	MODAL VECTOR THREE
6001	6144	AVAILABLE

FOURTH WORK TRACK

1	3000	MODAL VECTOR FOUR
3001	6000	MODAL VECTOR FIVE
6001	6144	AVAILABLE

FIFTH WORK TRACK

1	3000	MODAL VECTOR SIX
3001	6000	MODAL VECTOR SEVEN
6001	6144	AVAILABLE

SIXTH WORK TRACK

1	3000	MODAL VECTOR EIGHT
3001	6000	MODAL VECTOR NINE
6001	6144	AVAILABLE

SEVENTH WORK TRACK

1	3000	MODAL VECTOR TEN
3001	6144	AVAILABLE

EIHGTH WORK TRACK

1	4010	ACOUSTIC MODEL ARRAYS
4011	6144	AVAILABLE

NINTH WORK TRACK

1	4010	ACOUSTIC MODEL ARRAYS
4011	6144	AVAILABLE

TENTH WORK TRACK

1	4010	ACOUSTIC MODEL ARRAYS
4011	6144	AVAILABLE

ELEVENTH WORK TRACK

1	4010	ACOUSTIC MODEL ARRAYS
4011	6144	AVAILABLE

TWELVETH WORK TRACK

1	4608	MEASUREMENT DIRECTORY
4609	6144	AVAILABLE

THIRTEENTH WORK TRACK

1	3072	DISPLAY/BUFFER ARRAYS
3073	6144	AVAILABLE

ACOUSTIC MODAL STRUCTURE

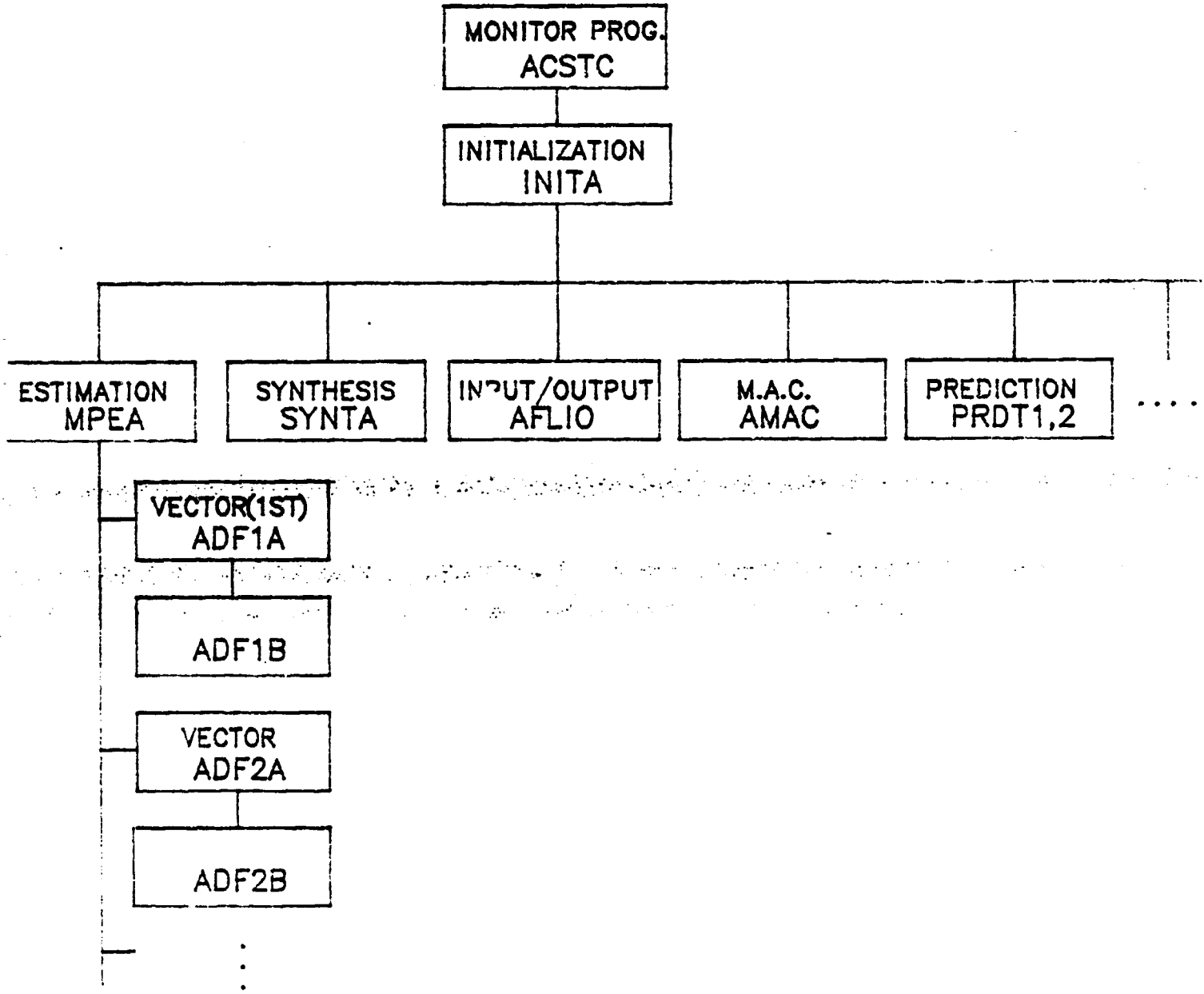

ACKNOWLEDGEMENTS

The autors would like to acknowledge the technical support of the staff and facilities of the University of Cincinati.

REFERENCES

1. S.N. Rschevkin , "Theory of sound", Pregamon Press 1963

2. Philip M. Morse and K. Uno Ingard "Theoretical Acousticcs", Mcgraw-Hill Book Co. 1968

3. E. Skudrzyk " The Foundations of Acoustics", Springer-Verlag ,1971

4. D.L. Brown ,R.J. Allemang ,R. Zimmerman and M. Mergeay "Parameter Estimation Techniques for MOdal Analysis" SAE Paper 790221 1979

5. P. Sas and R. Snoeys, "Prediction of the Intensity Based on Mode Shape" 1st IMAC 1982

6. W.G. Halvorsen and D.L. Brown, "Impulse Technique for Structural Frequency Response Testing" Sound and Vibration ,1977

7. A.L.Klosterman, "On the Experimental Determination and Use of MOdal Representation of Dynamic Characteristics", Ph.D dissertation, Univ.of Cincinnati Univ. of Cincinnati, 1971

8. N. Okubo, "Modal Analysis of Machinery", Chuo Univ. 1982

9. "Modal Analysis -Short Course Notes" , Dept. of Mechanical Engineering, Univ. of Cincinnati, 1981

10. Hayes